Consistent Rice Information for Sustainable Policy (CRISP)

Products Validation Report

(IRRI)

November 2025

Versions

Version:	1.0
Date:	09/07/2025
Changes:	-

Version:	2.0
Date:	15/09/2025
Changes:	Add preliminary results over test sites

Version:	3.0
Date:	30/11/2025
Changes:	Document Finalization

Table of Contents

1. Purpose

The document provides the validation results of the rice mapping products generated by the CRISP project over five pilot sites:

1) Andhra Pradesh State, India;

2) Mwea Irrigation Scheme, Kenya;

3) Luzon, Philippines;

4) Kano State, Nigeria;

5) Senegal River Valley, Senegal.

In line with the above-mentioned rationale, the document is structured as follows:

- Chapter 2 provides the context for the validation of the CRISP products;
- Chapter 3 provides the validation results for Andhra Pradesh State, India;
- Chapter 4 provides the validation results for Mwea Irrigation Scheme, Kenya;
- Chapter 5 provides the validation results for Luzon, Philippines;
- Chapter 6 provides the validation results for Kano, Nigeria;
- Chapter 7 provides the validation results for Senegal River Valley, Senegal;
- Chapter 8 summarizes the validation results, considering all sites;
- Chapter 9 provides the conclusion of the validation exercise.

2. Validation of rice products generated by the CRISP platform

This validation exercise is undertaken for five test sites, covering various rice ecosystems (rainfed, irrigated), geographic regions (east and west Africa, South Asia, and South-East Asia), and production systems across the world, including various levels of intensification (Figure 2.1):

1) Andhra Pradesh State, India (rainfed, irrigated);

2) Mwea Irrigation Scheme, Kenya (irrigated);

3) Luzon, Philippines (rainfed, irrigated);

4) Kano State, Nigeria site (rainfed, irrigated);

5) Senegal River Valley, Senegal site (irrigated).

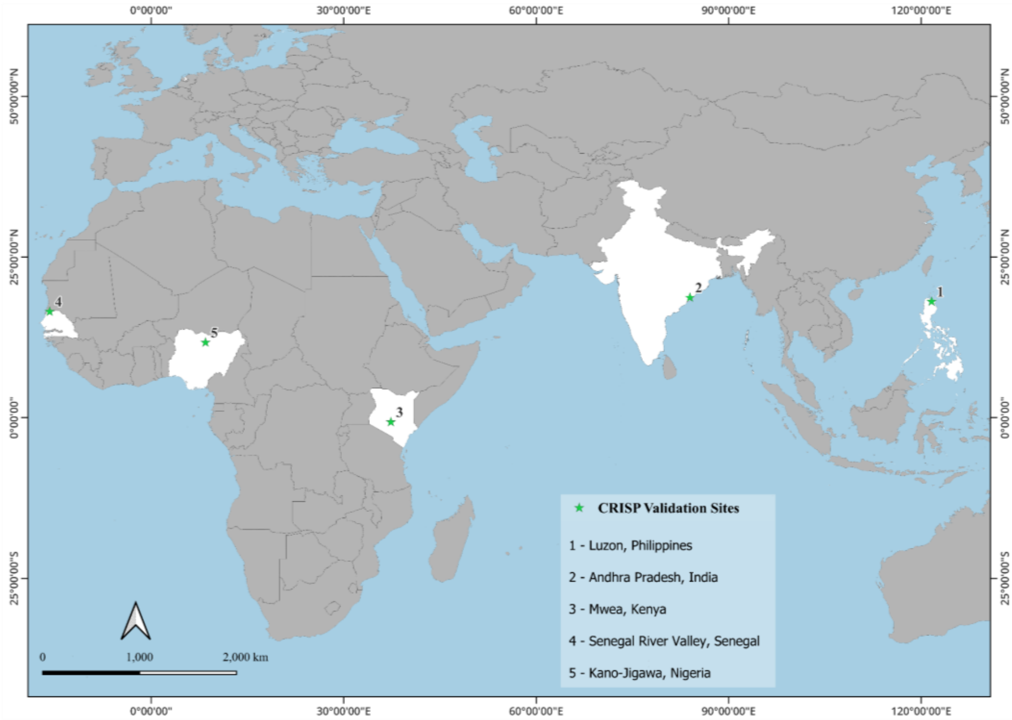

Figure 2.1. Geographic localization of the five sites used to test the CRISP rice mapping platform

The product to be validated include the rice area and yield, and the impacts of flood and drought events on rice area and/or yield (Table 2.1). The validation analysis is based on various datasets (Table 2.2):

- Data collected in the field during the seasons under investigation;
- Government and literature data or statistics;
- Published rice area or production maps.

It is important to note that no field data have been specifically collected for this CRISP validation exercise, due to funding limitation. Field data when available, have been collected as part of earlier CGIAR IRRI projects undertaken at the test sites. The Start-of-Season products were not validated due to the lack of planting or sowing reference datasets.

Table 2.1. Products to be validated for the five test sites

Sites	Season	Product
Kenya, Mwea	Main Season 2023	Rice Area, Yield
Senegal, Senegal River Valley	Wet Season 2023	Rice Area, Yield
Nigeria, Kano	Wet Season 2023	Rice Area, Yield
Philippines, Luzon	Wet Seasons 2017-18 and 2018-19	Rice Area, Yield
India, Andhra Pradesh	Wet season 2018	Rice Area, Flood Area

Table 2.2. Data sources for the validation of the rice CRISP products

Sites	Rice Area	Yield
Kenya, Mwea	• Ground validation point • NIA-MIAD data, Kenya	• Crop Cut Experiments (field) • NIA-MIAD data, Kenya
Senegal, Senegal River Valley	• Ground validation point • SAED and ISRA data	• Crop Cut Experiments (field) • SAED and ISRA data
Nigeria, Kano	• Ground validation point	• Farmer's field yield data
Philippines, Luzon	• Photo interpreted point • Government data	• Government data
India, Andhra Pradesh	• Ground validation data	NA

NIA-MIAD National Irrigation Authority - Mwea Irrigation Agricultural Development (MIAD) Centre; ISRA Institut Sénégalais de Recherche Agricole, SAED Société d'Aménagement et d'Exploitation des Terres du Delta du Fleuve Sénégal

The processes, data, and algorithm used to generate the rice CRISP products are described in the Technical Specification document released by the CRISP team in January 2025. The processing chain includes the following pipelines or modules:

- The Sentinel-1 Intensity and Sentinel-2 Pre-Processing Pipeline consisting of the European Space Agency (ESA) SNAP 12 toolbox;

- Slope and Sentinel-1 Vegetation Indices pipeline using sarmap's proprietary IP to generate a SAR-derived index, EDPSVI;

- The Rice Area Mapping and Start of Season (SoS) Detection Pipeline using sarmap's proprietary IP to integrate SAR multi-temporal acquisitions (polarization, EDPSVI) with optical vegetation indices (e.g., NDVI) to identify rice temporal signatures and detect the Start of Season (SoS);

- Leaf Area Index (LAI) Processor leveraging sarmap's proprietary IP to generate the Leaf Area Index (LAI) by combining temporal Sentinel-1 vegetation indices with geospatial data;

- The Yield Modelling Processor integrating the ORYZA V3 yield simulation model, developed by the International Rice Research Institute (IRRI), to model rice growth, development, and yield;

- The Multi-Temporal Feature Extraction Pipeline using sarmap's proprietary IP to derive first-order statistical features from SAR and optical data time series for segmentation and classification tasks;

- The yield modelling component uses remote sensing-derived layer (including Rice Area, Start-of-Season, and Leaf Area Index), as well as other data on weather, soil, variety, and crop management. The data / parameter used for the various sites are listed in Table 2.3.

Table 2.3. Data and parameters used for the yield modelling in each site and the source of the data

Sites	Weather$	Soil&	Variety (dominant)#	Crop management
Kenya, Mwea	Copernicus AgERA5 satellite weather data	Soil parameters analysed from soil samples (NIA-MIAD[1])	Basmati 370	Farmer surveys Nitrogen fertilization: 80 kg, irrigated condition with transplanted rice
Senegal, Senegal River Valley	Copernicus AgERA5 satellite weather data	Soil parameters analysed from soil samples (ISRA[2])	Sahel 108	ISRA team Nitrogen fertilization: 120 kg, irrigated condition with transplanted rice
Nigeria, Kano	Copernicus AgERA5 satellite weather data	Soil parameters derived from ISRIC - World Soil Information database	Faro calibrated for rainfed and irrigated conditions	Africa Rice team Rainfed: nitrogen fertilization: 80 kg, rainfed condition with transplanted rice Irrigated: nitrogen fertilization 80-120kg (wet season) irrigated condition with transplanted rice
Philippines, Luzon	NASA and CHIRPS (rainfall) satellite weather data	Soil parameters derived from ISRIC - World Soil Information database	MTR110 variety, calibrated based on maturity duration of 110 days	PhilRice team Irrigated: nitrogen fertilization: 90 kg (dry season), irrigated condition with transplanted rice
India, Andhra Pradesh	NASA and CHIRPS (rainfall) satellite weather data	Soil parameters derived from ISRIC - World Soil Information database	MTU1001	Secondary data and local knowledge Nitrogen fertilization: 80 kg, irrigated condition with transplanted rice

[1] NIA-MIAD National Irrigation Authority - Mwea Irrigation Agricultural Development (MIAD) Centre, [2] ISRA Institut Sénégalais De Recherche Agricole, [$] Weather data: required Temperature (max, min), solar radiation, vapor pressure, wind speed, rainfall, [&] Soil data: Physical (texture and particle size, bulk density), chemical (pH, organic matter, organic carbon, organic nitrogen, total nitrogen), and hydrological (saturated hydraulic conductivity, saturated volumetric water content, volumetric water content at field capacity, volumetric water content at wilting point, volumetric water content at air dryness). [#] Variety: Yield is generated for a dominant rice variety.

3. Validation of the Andhra Pradesh, India Site

3.1. Site

Rice is a major cereal crop and staple food in eastern and southern India, where most farmers depend solely on rice for their livelihood. In India, about half of the total area under rice crops is irrigated and is grown in bunded fields. Other rice crops are grown under rainfed upland and lowland systems, with diverse soil and climatic conditions. The lowland system can be favourable, drought-prone, or submergence-prone. In some areas, rice is cultivated in flood-prone ecosystems, where flood is an integral part of the system, which requires specific cropping techniques. The State of Andhra Pradesh (Figure 3.1.) is situated along the Bay of Bengal Coast in the southeastern part of India. Andhra Pradesh is characterised by a semi-arid, moist to dry, sub-humid climate, and has approximately 4 million hectares under rice, which is mainly irrigated (40% of the cultivated area). The rice is grown in the Kharif (wet) season from June to October/ November and in the Rabi (dry) season from October to April. Two types of crop establishment methods are normally used: direct seeded and transplanting. The average productivity is about 3 tonnes/ha. The major constraints in production are biotic stresses such as bacterial leaf blight, gall midge and sheath blight and abiotic stresses like water scarcity, recurrence of droughts and severe cyclonic storms and floods, low fertility red lateritic and black soil, with salinity issues, especially in coastal districts. In 2019, during July to September, Andhra Pradesh (with 13 other Indian states) was affected by widespread flooding, due to excessive rains and overflow of the Godavari River. It was the heaviest monsoon in the last 25 years. Excessive water affected approximately 180,000 hectares of Kharif (wet season) crops, including essential crops like paddy rice, maize, soybean, cotton, pulses. Main damages resulted from water logging, pest outbreaks, and fungal diseases, causing significant yield losses.

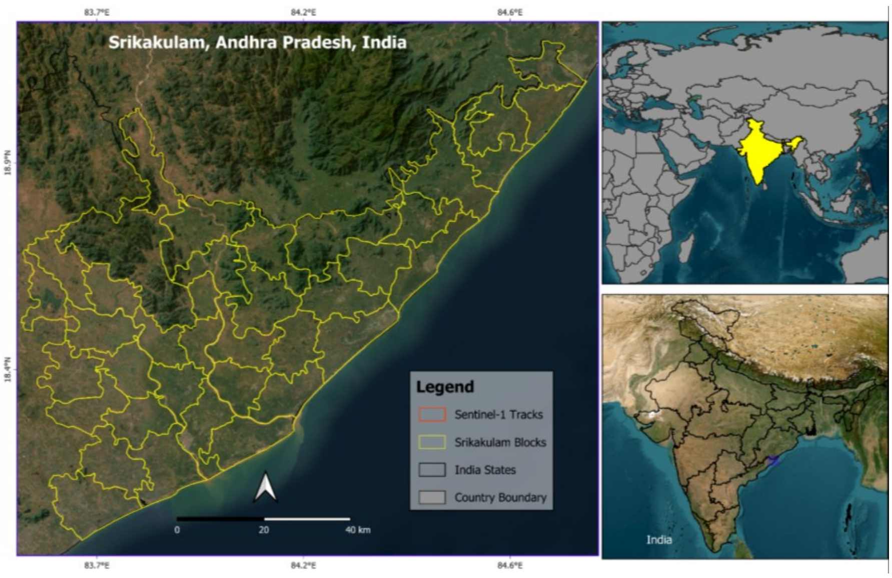

Figure 3.1. The Srikakulam district of Andhra Pradesh, India

3.2. Rice CRISP products

As part of the CRISP workflow, three rice-related products were derived for the Andhra Pradesh site: the rice area (RA), the Start-of-Season (SoS), and the flood extent for the 2018 wet season. The flood product was generated with Sentinel-1 data acquired pre flood and TerraSAR-X data acquired post flood. No rice yield was generated for this site. The products are shown in Figures 3.2–3.4.

3.2.1. Rice Area

The total rice area mapped by the CRISP algorithm in the Srikakulam district during the 2018 Kharif (wet) season was 214,181 ha (Figure 3.2). The overall distribution reflects a concentration of rice cultivation in the central and coastal parts of the district, supported by irrigation infrastructures (canals, tanks and bore holes), or significant seasonal rainfall in rainfed lowlands. The largest rice areas were recorded in Jalumuru, Narasannapeta, Kothuru, Pathapatnam, and Tekkali blocks, each exceeding 8,000 ha (Table 3.1), while smaller areas (<3,000 ha) occurred in Kaviti, Laveru, and Vangara bloks which are smaller or having other Kharif crops such as groundnut, sugarcane, oilseeds, cashew. Spatial variations highlight the influence of topography and irrigation infrastructure on the extent of rice cultivation across the district.

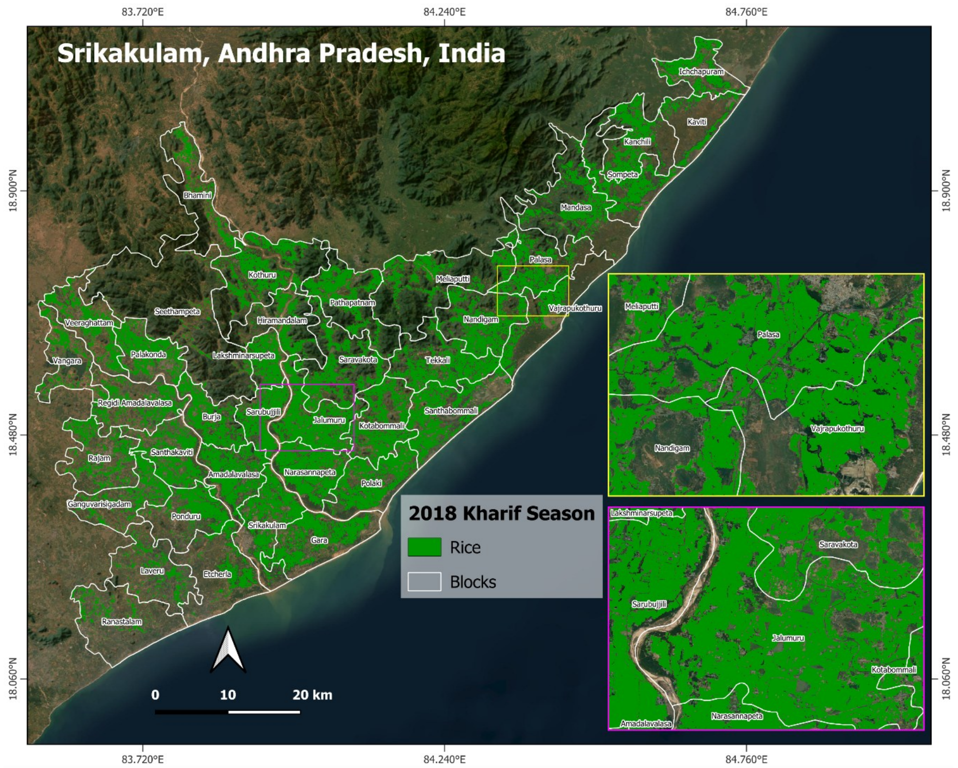

Figure 3.2. Spatial distribution of CRISP-derived rice area across the Srikakulam district, Andhra Pradesh, India for the 2018 Kharif (wet) season

3.2.2. Start of Season

The start-of-season (SoS) analysis indicated that rice establishment followed the onset of the south-west monsoon (Figure 3.3 and Table 3.1). The rice area expanded sharply from June (13,279 ha; 6.2%) to July (75,763 ha; 35.4%), reaching its maximum in August (124,303 ha; 58.0%), when most transplanting occurred. Only a small portion of fields (836 ha; 0.4%) was sown in September, representing late-season rice which might be planted in rainfed lowland or tail-end of canal irrigated rice fields. The SoS distribution suggests that about 93% of rice in Srikakulam was established between July and August, reflecting the district's strong dependence on monsoon rainfall and irrigation scheduling for timely field preparation and planting.

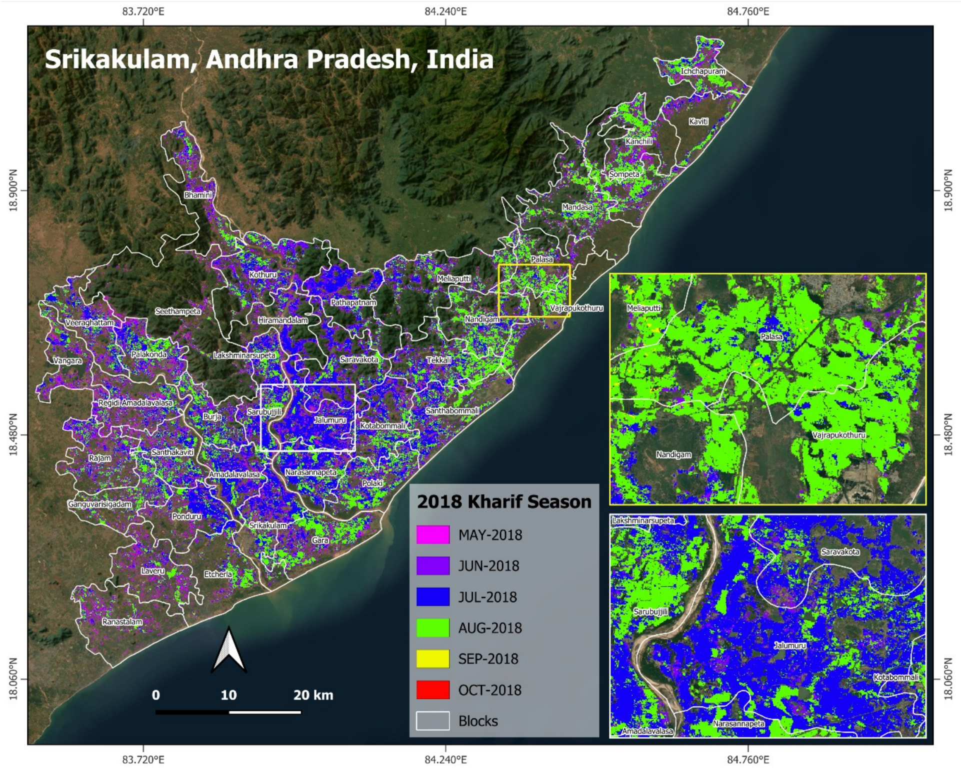

Figure 3.3. Start-of-Season spatial distribution of CRISP-derived rice area across the Srikakulam district, Andhra Pradesh, India for the 2018 Kharif (wet) season

Table 3.1. Start of season-wise rice area estimates in Srikakulam district, 2018 Kharif (wet) season

Block	June	July	August	September	Total
Amadalavalasa	239	4386	2640	14	7279
Bhamini	79	836	1997	3	2915
Burja	345	1298	3815	9	5467
Etcherla	158	578	2413	13	3162
Ganguvarisigadam	46	690	3860	47	4642
Gara	328	1472	5652	9	7461
Hiramandalam	351	2041	654	1	3047
Ichchapuram	399	983	3734	2	5118
Jalumuru	546	7516	1789	6	9856
Kanchili	995	133	5031	2	6161
Kaviti	308	513	1395	2	2219
Kotabommali	185	4372	3375	20	7952
Kothuru	1528	2185	3887	4	7605
Lakshminarsupeta	36	2118	1780	36	3969
Laveru	370	738	1674	31	2814
Mandasa	557	228	5146	143	6075
Meliaputti	572	1034	4274	52	5933
Nandigam	170	1489	6428	13	8101
Narasannapeta	170	4923	3346	1	8441
Palakonda	433	1621	3756	1	5811
Palasa	307	305	4837	65	5514
Pathapatnam	620	4167	1661	13	6461
Polaki	67	3081	5063	69	8279

Ponduru	230	3154	1588	28	5000
Rajam	115	1285	3379	37	4816
Ranastalam	304	214	1508	12	2039
Regidi Amadalavalasa	418	984	3465	45	4912
Santhabommali	157	3457	4916	47	8576
Santhakaviti	92	2296	4127	20	6535
Saravakota	459	4860	2251	8	7578
Sarubujjili	595	2456	2631	1	5683
Seethampeta	165	370	1309	11	1855
Sompeta	830	167	4408	14	5420
Srikakulam	190	4071	3060	7	7329
Tekkali	356	2422	5605	39	8421
Vajrapukothuru	62	354	3542	5	3963
Vangara	305	1016	1444	3	2768
Veeraghattam	192	1949	2863	1	5004
Srikakulam District	13279 (6.2%)	75763 (35.4%)	124303 (58.0%)	836 (0.4%)	214181

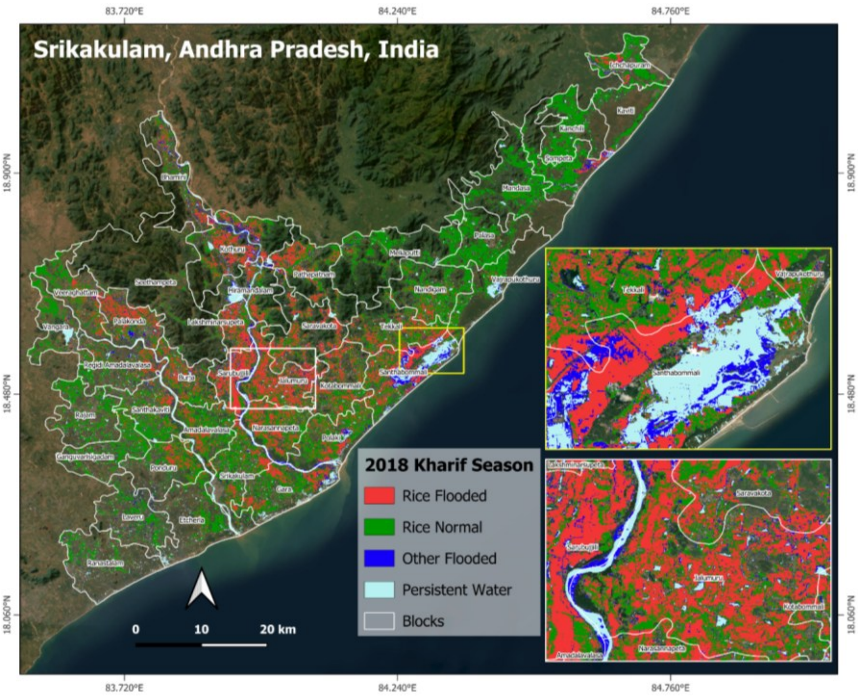

Figure 3.4. Spatial distribution of flood-affected and rice-flooded areas in Srikakulam District during the 2023 Kharif (wet) season derived from CRISP flood maps

3.2.3. Area affected by flood

Flooding was most common in the central and eastern parts of the district, especially near the Vamsadhara River and its irrigation network. Overlaying the rice map with the flood map showed that around 72,105 ha (33.7%) of rice area was flooded for at least three days during the season (Table 3.2), as detected from the TerraSAR-X satellite image acquired close to the cyclone event. The remaining 142,077 ha (66.3%) of rice fields were reported as non-flooded. The highest flooded rice areas reported (>50%) were in Santhabommali, Kothuru, Pathapatnam, and Jalumuru blocks, located in lowland and river basins. In contrast, Kanchili, Mandasa, and Laveru had less than 5% flooded rice, mainly due to their upland terrain position and limited water retention capacity.

Table 3.2. Total flooded and rice-flooded area in Srikakulam district during the 2023 Kharif (wet) season

Block	Total Rice Area (ha)	Flooded Rice (ha & %)	Rice Not Flooded (ha)
Amadalavalasa	7279	2438 (33.5)	4841
Bhamini	2915	1116 (38.3)	1799
Burja	5467	2433 (44.5)	3034
Etcherla	3162	376 (11.9)	2786
Ganguvarisigadam	4642	433 (9.3)	4209
Gara	7461	2747 (36.8)	4714
Hiramandalam	3047	1493 (49.0)	1554
Ichchapuram	5118	905 (17.7)	4213
Jalumuru	9856	6427 (65.2)	3429
Kanchili	6161	73 (1.2)	6088
Kaviti	2219	183 (8.2)	2038
Kotabommali	7952	3789 (47.6)	4163
Kothuru	7605	4307 (56.6)	3298
Lakshminarsupeta	3969	2567 (64.7)	1403
Laveru	2814	77 (2.7)	2737
Mandasa	6075	114 (1.9)	5961
Meliaputti	5933	385 (6.5)	5548
Nandigam	8101	1689 (20.8)	6412
Narasannapeta	8441	3930 (46.6)	4511
Palakonda	5811	3374 (58.1)	2437
Palasa	5514	120 (2.2)	5394
Pathapatnam	6461	3147 (48.7)	3314
Polaki	8279	2735 (33.0)	5545
Ponduru	5000	1421 (28.4)	3579
Rajam	4816	372 (7.7)	4444
Ranasthalam	2039	74 (3.6)	1965
Regidi Amadalavalasa	4912	1616 (32.9)	3296
Santhabommali	8576	4657 (54.3)	3919
Santhakaviti	6535	1596 (24.4)	4939
Saravakota	7578	4433 (58.5)	3145
Sarubujjili	5683	4189 (73.7)	1494
Seethampeta	1855	327 (17.6)	1527
Sompeta	5420	646 (11.9)	4774
Srikakulam	7329	2203 (30.1)	5126
Tekkali	8421	3709 (44.0)	4712
Vajrapukothuru	3963	465 (11.7)	3498
Vangara	2768	181 (6.5)	2588
Veeraghattam	5004	1465 (29.3)	3539
Srikakulam District	**214181**	**72105 (33.7)**	**142077 (66.3)**

3.3. Data used for CRISP products validation

A total of 178 ground reference points were collected across the Srikakulam district during the 2018 Kharif season (Figure 3.5). The points were acquired during two different periods. The first set comprised rice and non-rice fields collected during the mid-season to validate the rice area map. Since rice is the dominant crop during the wet season in Srikakulam, the field team could only collect a limited number of non-rice crop points (mainly cotton and maize). To balance the rice versus non-rice dataset, additional non-rice points representing permanent non-rice land covers such as cashew and coconut plantations and barren land were added and photo interpreted from very high-resolution images. The second set of points was collected immediately after the cyclone event, targeting flooded and non-flooded rice and non-rice fields to validate the flood extent map. All ground truth points were independent of the calibration dataset used in CRISP product generation and were used exclusively for validation.

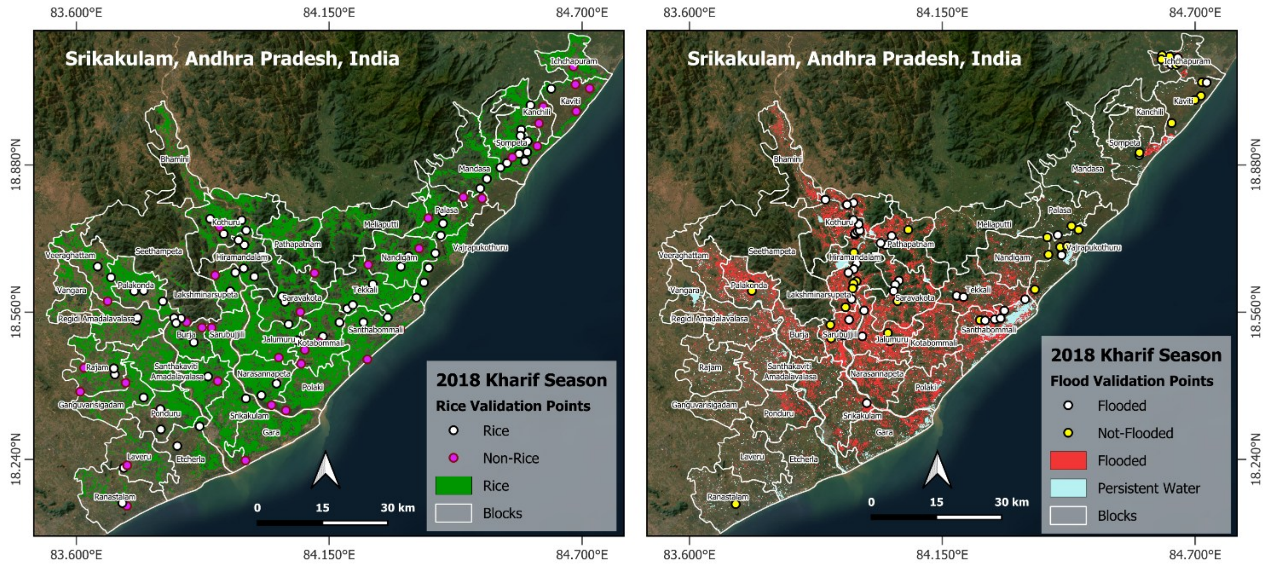

Figure 3.5. Distribution of collected ground truth points across Srikakulam district used for validation of CRISP rice area and flood maps during the 2018 Kharif season.

3.4. Results of CRISP products validation

3.4.1. Rice area

The rice classification map generated by the CRISP algorithm achieved a high overall accuracy of 94.2% and a Kappa index of 0.88, indicating strong agreement with field observations (Table 3.3). Rice fields were mapped with both producer's and user's accuracy of 95.5%, while non-rice fields achieved producer's and users' accuracy of 91.9%. The classification demonstrates excellent consistency across classes, with only minimal misclassification between rice and non-rice areas. Some isolated misclassified pixels were visible along field boundaries or in mixed-cropping zones, giving a slight salt-and-pepper appearance; however, these minor errors did not significantly affect the overall rice extent estimation.

Table 3.3. Confusion matrix for the CRISP rice area and flood classifications, 2018 Kharif season, Srikakulam district.

CRISP Rice map					**CRISP Flood map**				
Predicted class from the map					Predicted class from the map				
		Rice	**Non-rice**	**Accuracy**			**Flood**	**Non-flood**	**Accuracy**
Actual class (survey)	**Rice**	64	3	95.5%	Actual class (survey)	**Flood**	35	7	83.3%
	Non-rice	3	34	91.1%		**Non-flood**	5	27	84.4%
	Reliability	95.5%	91.9%	94.2%		**Reliability**	87.5%	79.4%	83.8%
Average accuracy		93.7%			Average accuracy		83.9%		
Average reliability		93.7%			Average reliability		83.5%		
Overall accuracy		**94.2%**			**Overall Accuracy**		**83.8%**		
Kappa index		0.88			Kappa index		0.68		

3.4.2. Flood map

The validation of the CRISP-derived flood map showed an overall accuracy of 83.8% and a Kappa index of 0.68, indicating good agreement between satellite-derived flood extents and ground observations (Table 3.3). Flooded areas were mapped with a producer's accuracy of 83.3% and a user's accuracy of 87.5%, while non-flooded areas achieved a producer's accuracy of 84.4% accuracy. Most discrepancies occurred in areas affected by short-duration floods (less than 2 days) or partial submergence, which were not detected at the time of the satellite image acquisition. Despite these minor inconsistencies, the CRISP flood map effectively represented the spatial distribution and extent of inundation, especially within the major lowland and canal-irrigated areas of the district.

4. Validation of the Mwea, Kenya site

4.1. Site

Rice is one of Kenya's most important grains and has become a key staple food in urban areas. The quantity of rice produced nationally in 2019 was 80,000 tons, while consumption reached 710,000 tons, indicating that the rice consumption in Kenya is heavily reliant on international markets. Most of the rice production is irrigated and originates from eight irrigation schemes, amongst which the Mwea Irrigation Scheme is the most important with about 10000 ha. Mwea is in the Kirinyaga County, 100 km north-west of Nairobi, and south of Mount Kenya. It is the oldest and largest schemes among the four major gravity-based irrigation schemes in Kenya and produces 80% of the rice produced in the country. The scheme lies along the drainage basins of the rivers Nyamindi and Thiba which supply the irrigation water through gravity. The scheme practices two and half production seasons in a year: (1) a main season (July to December), and a ratoon crop (or regrowth) from December to February; and (2) a second season (March to July). Depending on weather conditions, the area being cultivated from March to July varies from 2000 to 4000 ha. The main varieties produced in MIS are Basmati 370, Komboka and newly introduced hybrid varieties i.e., Arize Tej Gold & Arize 6444 Gold. Yields typically varies between 5 and 6 t/ha.

4.2. Rice CRISP products

As part of the CRISP workflow, three rice-related products were derived for the Mwea site: the rice area (RA), start-of-season (SoS), and rice yield for the 2023 wet season (July–December). These products are shown in Figures 4.2–4.4.

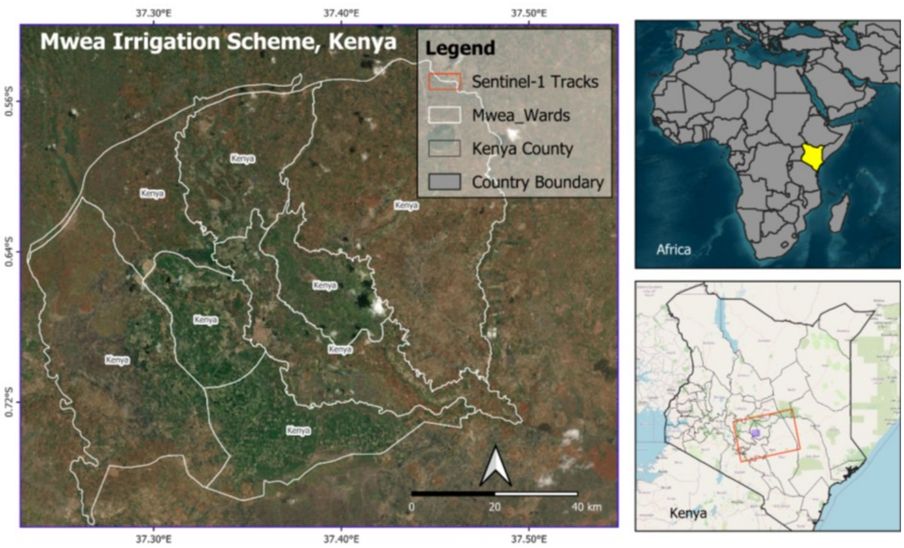

Figure 4.1. The Mwea Irrigated Scheme (MIS) site, Kenya

4.3. Rice CRISP products

As part of the CRISP workflow, three rice-related products were derived for the Mwea site: the rice area (RA), start-of-season (SoS), and rice yield for the 2023 wet season (July–December). These products are shown in Figures 4.2–4.4.

4.3.1. Rice Area

The CRISP-derived rice area map (Figure 4.2) shows that the total rice extent across the Mwea Irrigation Scheme (MIS) during the 2023 main season was 12,231 ha (Table 4.1). Rice cultivation was heavily concentrated in the southern and central blocks, particularly Wamumu (4,076 ha) and Thiba (2,615 ha), which together contributed nearly 55% of the total rice area. These two wards form the core production zones of MIS, which might benefit from a stable irrigation supply and well-established canal infrastructure. Substantial rice area was also mapped in Gathigiriri (1,935 ha) and Mutithi (1,781 ha), located on the eastern and western sides of the scheme, respectively. Moderate extents were observed in Tebere (1,183 ha) and Kangai (293 ha), while smaller, more fragmented fields were detected in Murinduko (117 ha) and Nyangati (231 ha). This spatial pattern possibly reflects the hierarchical water distribution within MIS, where upstream and centrally located wards typically receive more reliable irrigation flows than those at the MIS boundary area.

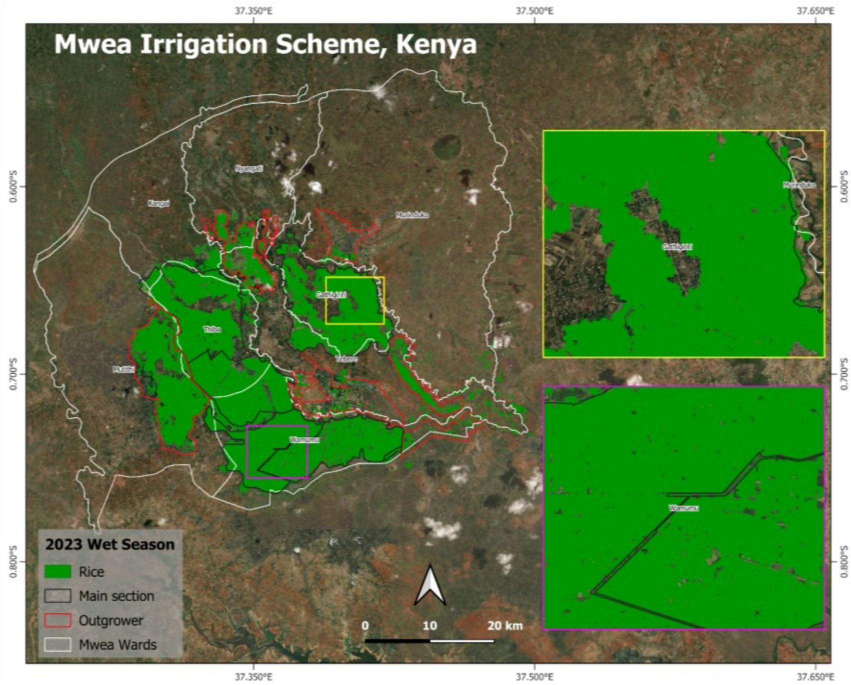

Figure 4.2. Spatial distribution of CRISP-derived rice area, Mwea Irrigated Scheme, 2023 main season

4.3.2. Start of Season (SoS)

The CRISP-derived SoS product (Figure 4.3) reveals a clear temporal pattern in planting across MIS. July was the dominant planting month, accounting for 5,435 ha (44.4%), indicating that nearly half of the scheme began transplanting early in the season. September plantings represented the second-largest share at 4,710 ha (38.5%), while August plantings covered 2,087 ha (17.1%) (Table 4.1). At the ward level, early planting was most prominent in Mutithi (56.5%), Thiba (56.4%), and Wamumu (40.4%), reflecting coordinated irrigation scheduling, timely land preparation, and early access to water in these blocks. Conversely, Nyangati (72.3%), Tebere (56.0%), and Murinduko (45.3%) showed predominantly late (September) planting. These delays may reflect water allocation constraints in downstream or tail-end sections of the irrigation network or slower field preparation in smaller, fragmented holdings. The spatiotemporal variability captured by CRISP highlights the operational dynamics of MIS, where planting schedules differ across irrigation blocks depending on water delivery timing, canal proximity, and management practices.

Table 4.1. Ward-wise rice area (ha, %) by start-of-season month and rice yield (t/ha) derived from CRISP products for Mwea, 2023 main season

Wards	SoS date-wise Rice Area in ha and (%)				Rice Yield (t/ha)
	Jul	Aug	Sep	Total	
Gathigiriri	906 (46.8)	404 (20.9)	625 (32.3)	1935	4.44
Kangai	93 (31.7)	93 (31.7)	107 (36.5)	293	4.44
Murinduko	26 (22.2)	38 (32.5)	53 (45.3)	117	4.46
Mutithi	1,006 (56.5)	198 (11.1)	576 (32.3)	1781	4.45
Nyangati	8 (3.5)	55 (23.8)	167 (72.3)	231	4.45
Tebere	271 (22.9)	250 (21.1)	662 (56.0)	1183	4.45
Thiba	1,475 (56.4)	408 (15.6)	732 (28.0)	2615	4.45
Wamumu	1,648 (40.4)	640 (15.7)	1,788 (43.9)	4076	4.47
Mwea Total	**5,435 (44.4)**	**2,087 (17.1)**	**4,710 (38.5)**	**12231**	**4.45**

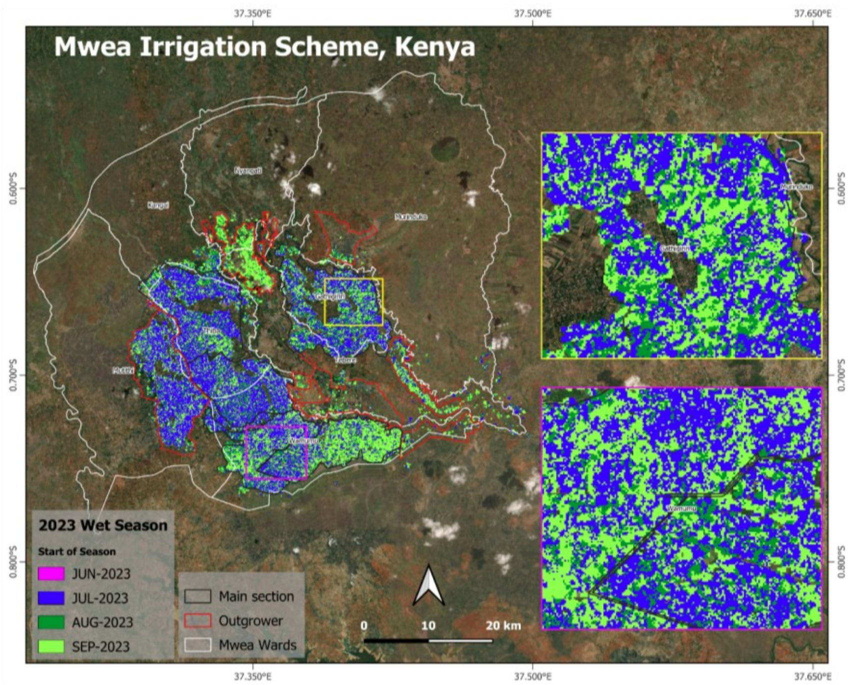

Figure 4.3. Start of season (SoS) distribution of rice fields in Mwea Irrigated Scheme (MIS) for the 2023 wet season.

4.3.3. Rice Yield

The CRISP-estimated yield map (Figure 4.4) showed a uniform yield distribution across the Mwea region, with an average of 4.45 t/ha (Table 4.1). Yields were consistent across most wards, varying only between 4.44 and 4.47 t/ha. This suggests uniform agronomic performance and water availability during the wet season. In addition, the site extents over a relatively small area (10x10 km), with small variability in weather and soil conditions, while settings are used for a dominant variety and general agronomic / crop management. This may also explain some limited yield variability recorded in the yield model over Mwea. Overall, the yield patterns indicate stable production levels across Mwea, consistent with the controlled irrigation practices of the National Irrigation Authority.

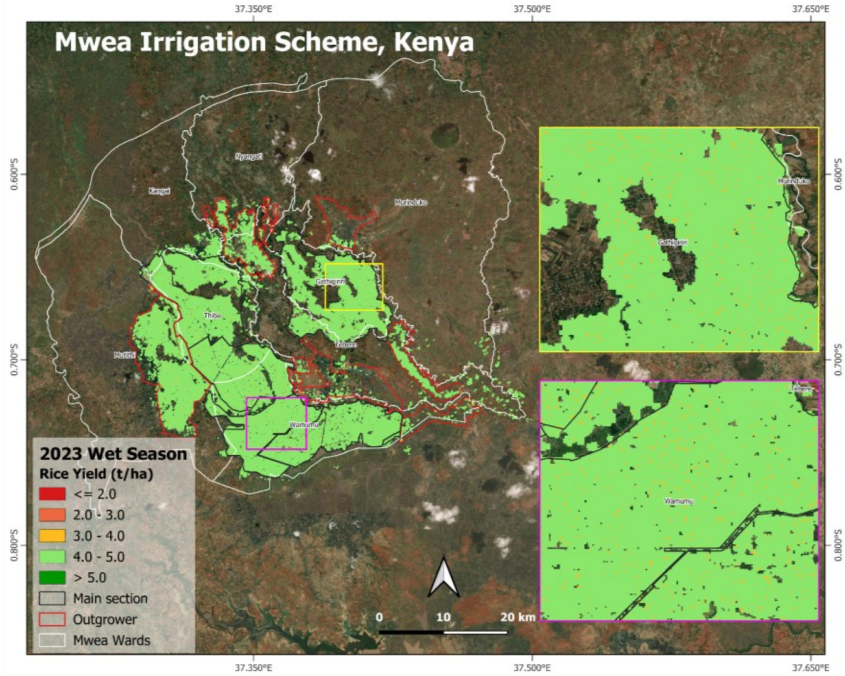

Figure 4.4. CRISP-derived rice yield distribution for Mwea Irrigated Scheme during the 2023 main season

4.4. Data used for CRISP products validation

A total of 109 ground truth points were collected across the irrigation scheme area, comprising 77 rice and 32 non-rice samples (Figure 4.5). As the region is only irrigated, rice fields occupied most of the area during the 2023 main season. Non-rice fields were generally small, limited and primarily located along the outer boundaries of the main irrigation parcels. Non-rice plots were mainly planted with maize, along with a few vegetable crops such as tomato and beans. In addition to the field validation dataset, 60 crop cutting experiments or CCEs were conducted at rice maturity across the irrigation scheme. These CCE observations served as an independent reference for validating the CRISP-derived rice yield map for the 2023 main season.

4.5. Results of CRISP products validation

4.5.1. Rice area

The classification achieved an overall accuracy of 92.7% and a Kappa index of 0.85, indicating a very strong agreement with the field data (Table 4.2). Rice fields were mapped with 93.5% accuracy, while non-rice areas achieved 90.6% accuracy, reflecting a well-balanced performance across both classes. The CRISP platform exhibited high-class reliability, with 96.0% user's accuracy for rice and 85.3% for non-rice, demonstrating some limited rice omission and strong discrimination of non-rice features in the MIS. The 12,231 ha of planted rice recorded by CRISP in MIS is coherent with the estimate generated by the National Irrigation Authority which identified 11655 ha for the main season in 2023 (Vincent, Kipngetich, personal communication). CRISP would slightly overestimate the scheme of about 5%.

To further assess spatial consistency, the CRISP rice map was compared with the Africa 20 m rice map produced for the same 2023 wet season (Jiang et al., 2025). The Africa 20 m map showed substantially lower agreement with the validation field dataset, achieving an overall accuracy of 71.6%, and a Kappa of 0.43 (Table 4.3). This is primarily due to higher rice omission with only 50.9% of user's accuracy for the non-rice class. This high omission of rice fields is particularly noticeable in the eastern part of the scheme, such as the eastern section of the Wamumu Ward and the Gathigiriri Ward (Figure 4.6).

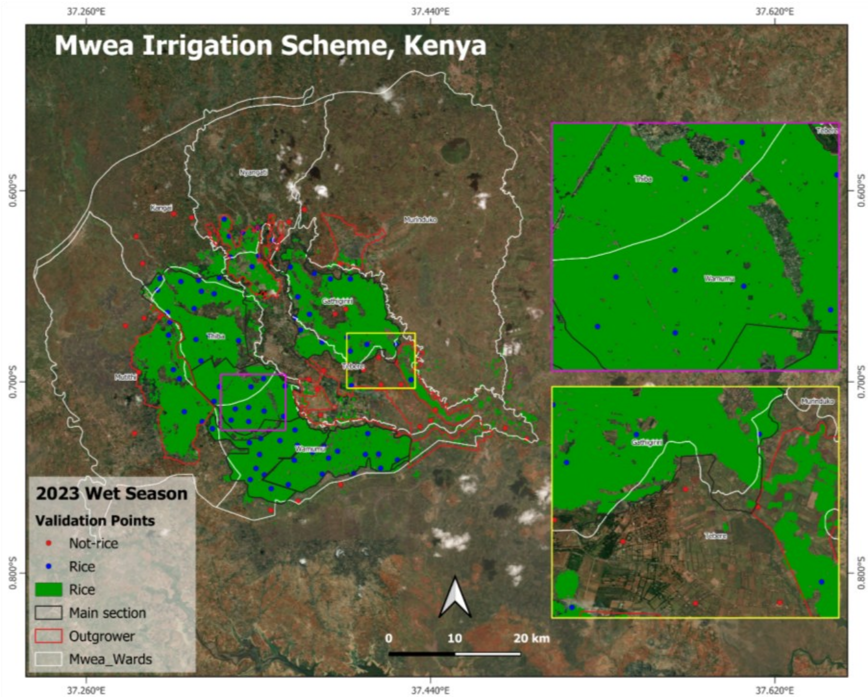

Figure 4.5. Spatial distribution of validation points (rice and non-rice) used for CRISP rice map validation in the Mwea Irrigated Scheme, 2023 main season.

Ward-level comparisons (Table 4.3) showed that the combined rice area detected by both maps was 13,114 ha, of which 7,270 ha (55.4%) were mapped by both products. The CRISP map uniquely identified 4,963 ha (37.8%), whereas the Africa 20 m product uniquely mapped 881 ha (6.7%). The strongest agreement occurred in Wamumu and Thiba, where more than half of the mapped area overlapped, reflecting greater consistency in core rice producing blocks. In contrast, wards such as Nyangati and Murinduko showed minimal overlap possibly due to more fragmented field patterns and mixed land cover that likely challenge the coarser continental-scale product. The Africa 20 m map missed large rice sections as evident in Figure 4.6, and in the comparison with the official boundaries of the scheme (Figure 4.7). In addition, the 20m Africa rice map identified rice patches in the western part of MIS, relatively far form the core MIS sections, and which are very unlikely to occur. Overall, the CRISP-derived rice map demonstrated a more accurate and spatially consistent delineation of rice extent than Jiang et al Africa 20m rice map. Its higher accuracy, stronger reliability, and better spatial alignment with known scheme boundaries (Figure 4.7) illustrate its suitability for local-scale monitoring and management applications.

Table 4.2. Confusion matrix for the rice area classification produced at the African continental level (Jiang et al. 2025) and in the Mwea Irrigated Scheme, wet season of 2023. Validation used the same 2023 field-collected points discussed in section 4.3.

CRISP Rice map					**Africa 20M Rice map (Jiang et al., 2025)**				
Predicted class from the map					Predicted class from the map				
		Rice	**Non-rice**	**Accuracy**			**Rice**	**Non-rice**	**Accuracy**
Actual class	**Rice**	72	5	93.5%	Actual class	**Rice**	49	28	63.6%

from survey					from survey				
	Non-rice	3	29	90.6%		**Non-rice**	3	29	90.6%
	Reliability	96.0%	85.3%	92.7%		**Reliability**	94.2%	50.9%	71.6%
Average accuracy		92.1%					77.1%		
Average reliability		90.6%					72.6%		
Overall accuracy		**92.7%**						**71.6%**	
Kappa index		0.85					0.43		

Table 4.3. Ward-wise comparison of rice area mapped by the CRISP rice map and the Africa 20 m rice map (Jiang et al., 2025) for the main season of 2023, and from Mwea Irrigated Scheme

Wards	Rice Area in ha and (%)			
	Only in CRISP	Only in Africa 20m	Both	Total
Gathigiriri	1,298 (67.0%)	4 (0.2%)	636 (32.8%)	1,938
Kangai	218 (70.1%)	17 (5.5%)	77 (24.8%)	311
Murinduko	112 (88.9%)	7 (5.6%)	6 (4.8%)	126
Mutithi	188 (8.2%)	510 (22.2%)	1,596 (69.6%)	2,293
Nyangati	229 (95.0%)	12 (5.0%)	0 (0.0%)	241
Tebere	1,020 (77.0%)	142 (10.7%)	163 (12.3%)	1,325
Thiba	489 (18.2%)	73 (2.7%)	2,127 (79.1%)	2,689
Wamumu	1,410 (33.6%)	116 (2.8%)	2,665 (63.6%)	4,191
Mwea Total	**4,963 (37.8%)**	**881 (6.7%)**	**7,270 (55.4%)**	**13,114**

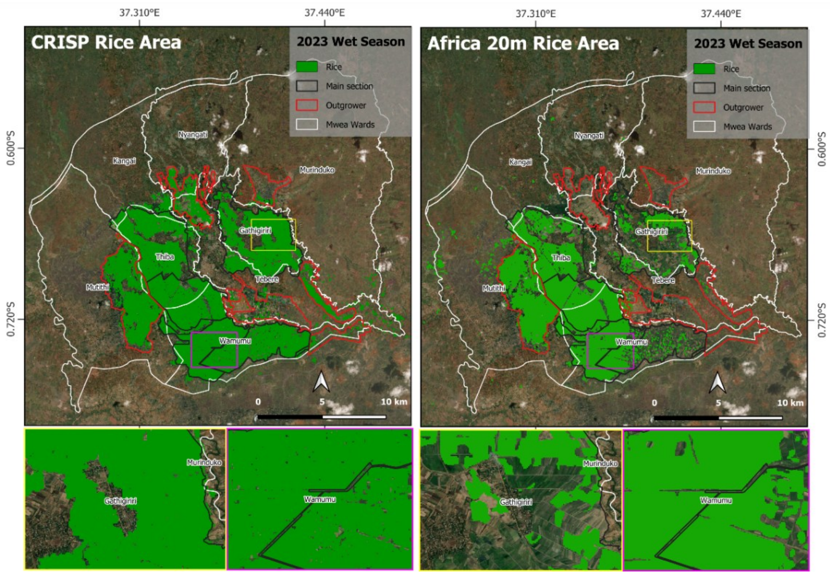

Figure 4.6. Rice area generated by the CRISP platform and the African continental level (Jiang et al., 2025) for the main season of 2023 in Mwea Irrigated Scheme

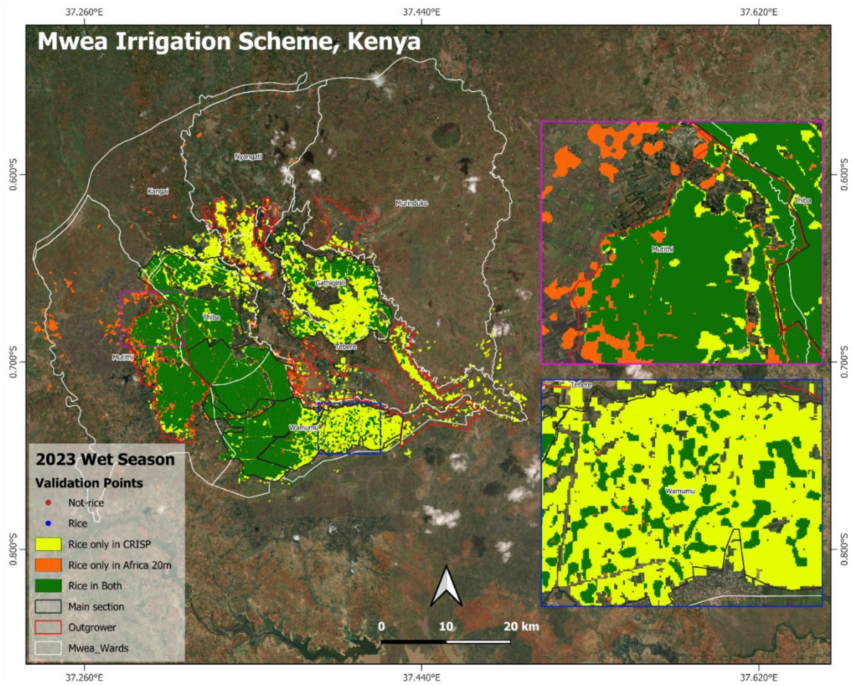

Figure 4.7. Comparison of the CRISP rice area map and rice area map produced at the African continental level by Jiang et al. (2025) for the main season of 2023 in Mwea Irrigated Scheme (MIS).

4.5.2. Rice area

The validation of the spatially-explicit yield generated by CRISP was carried out with 60 CCEs fields surveyed in the Mwea irrigation scheme during the main season 2023 (at harvest time). The CRISP yield estimates were compared with the CCE data, as shown in Table 4.4. Only 47 CCEs were used as some fields were affected by heavy crop lodging due to heavy rainfall and wind during the harvest and the crop cut exercise. No CCEs were available for the Kangai, Nyangati, Muthiti, and Murinduko Wards. The comparison between CRISP model yield estimates and actual CCE data across the four locations shows that the model generally underestimates rice yield. On average, CRISP predicts 4.47 t/ha, while the observed CCE yield is 5.28 t/ha, indicating an underestimation of about 0.81 t/ha. The NRMSE varied across wards, between 12 and 22%, and an average of 18%. The CCE yields generally had a higher range of variability from 4 to 7 t/ha across the fields, with an average of 5.2 t/ha.

Table 4.4. Comparison of rice yield CCEs with rice yield predicted in the Mwea Irrigated Scheme (MIS), during the 2023 wet season.

Location	No. Of CCE data	Average CRISP estimates (t/ha)	CCE data (t/ha)	RMSE (t/ha)	NRMSE (%)
Gathigiriri	9	4.44	5.40	0.96	22
Thiba	17	4.45	5.40	0.95	21
Wamumu	21	4.47	5.30	0.83	19
Tebere	1	4.45	5.00	0.55	12
AVERAGE	**47**	**4.47**	**5.28**	**0.81**	**18**

5. Validation of the Luzon, Philippines site

5.1. Site

The Philippines is an important rice producer ranking among the top 10 globally (20.06 million tons in 2023), but also a key importer to meet domestic demand. There are two major rice seasons in the country based on the amount of rainfall, the wet season from June to November and dry season from December to May. The estimated national average yield of paddy rice is around 4.2 t/ha with peaks up to 6-7t/ha. The major rice-producing regions are Central Luzon, Cagayan Valley, Eastern Visayas, and Bicol. The Philippines are vulnerable to drought and flood. At least 20 typhoons occur annually particularly during the wet season when most rice areas are planted. Most of the farmers produce irrigated lowland rice where the soil is soaked before ploughing, followed by harrowing, and transplanting of seedlings. Direct seeding is also practised during the dry season. During the dry season of 2018-19 the Philippines farmers were affected by a drought due to a weak El Niño event. Early signals started in October prior to the rice establishment and peaked in March and April 2019 with widespread drought conditions affecting over 75% of the provinces. Crop damages were estimated to amount around USD 157 million and crop production suffered a decrease of 20% across the country. Damages were particularly important in major agricultural regions like the Cordillera Administrative Region and parts of Central Luzon (Figure 5.1) and threatened food security for vulnerable farming households.

Figure 5.1. The Luzon site and Cagayan province, Philippines

5.2. Rice CRISP products

As part of the CRISP standard algorithm, rice products were generated for the Luzon site covering selected Municipalities for the dry season of 2017-18 and of 2018-19. Rice Area and yield were mapped for the Cagayan Province (Figures 5.2-5.3, 5.5). The dry season of 2017-18 served as a referenced year as it was not affected by drought conditions.

5.2.1. Rice Area

During the 2017-18 dry season, the total rice area across the selected municipalities of northern Luzon (Cagayan, Apayao, Kalinga, and Isabela provinces) was 88,312 ha (Figure 5.2 and Table 5.1). Larger rice areas were concentrated in municipalities situated along the Cagayan River, which generally have extensive irrigated lowlands compared to the hilly upland zones, where agricultural land is more restricted. The municipalities of Solana (11,269 ha), Aparri (7,864 ha), Amulung (7,427 ha), and Lasam (6,186 ha) accounted for the largest share of dry-season rice cultivation in 2017-18. The 2017-18 season was considered a normal year, with favourable conditions for crop establishment and sufficient water availability across most of the Cagayan Valley. In the 2018-19 dry season, the total rice area increased to 96,359 ha, reflecting an overall 9.1% expansion despite the occurrence of early season drought conditions (Figure 5.3). Municipalities situated near the Cagayan River, particularly Solana (11,882 ha), Aparri (10,281 ha), and Amulung (8,253 ha), continued to report the largest rice areas in 2018-19. Nearly all municipalities recorded an increase in rice area between the two seasons. While Aparri experienced the largest absolute increase (+2,417 ha; +30.7%), notable gains were also observed in municipalities with comparatively smaller rice areas. These include Pinukpuk (+105 ha; +16.2%), Piat (+216 ha; +29.6%), Santa Maria–Isabela (+194 ha; +47.3%), Pudtol (+316 ha; +41.7%), and Tuguegarao City (+310 ha; +46.5%).

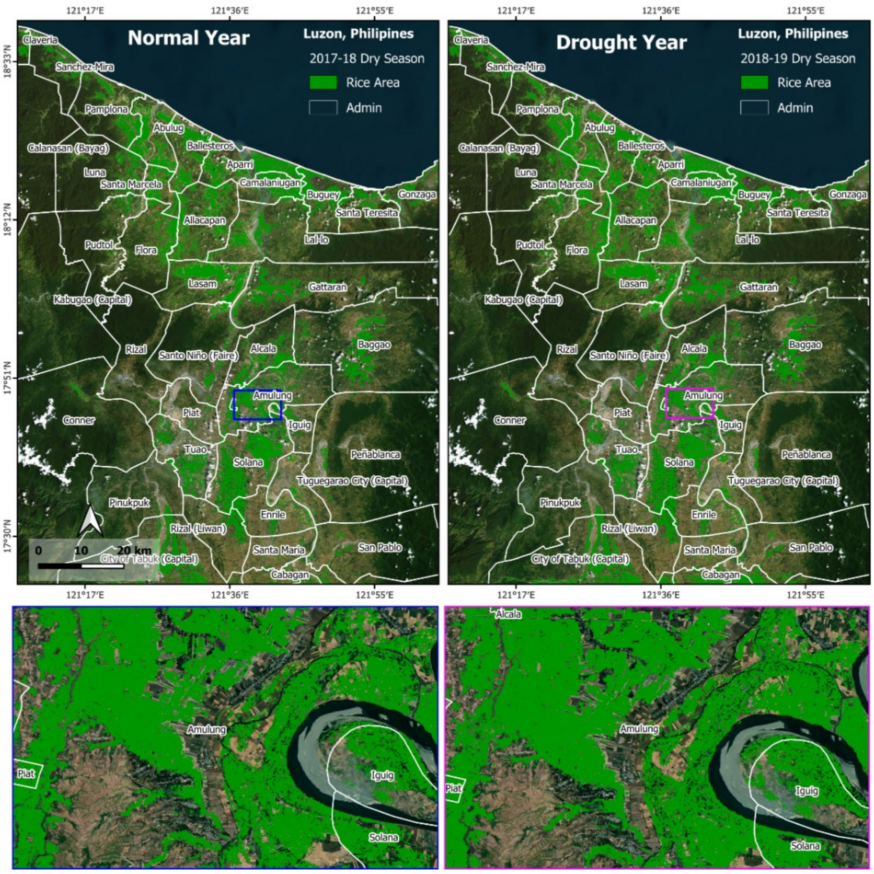

Figure 5.2. Rice area over the Cagayan Province in Luzon, Philippines, during the 2017–18 (normal year, left) and 2018–19 (drought year, right) dry seasons

Despite the early-season rainfall deficit in 2018-19 compared to the previous year (Figure 5.3), the total CRISP estimated rice area was slightly higher than in a normal year (2017-18), although the increase may also be mostly attributed to the margin error of the rice area extraction. It may in addition indicate the resilience of the rice cultivation in northern Luzon, which largely benefit from irrigated water from canals and shallow pumps.

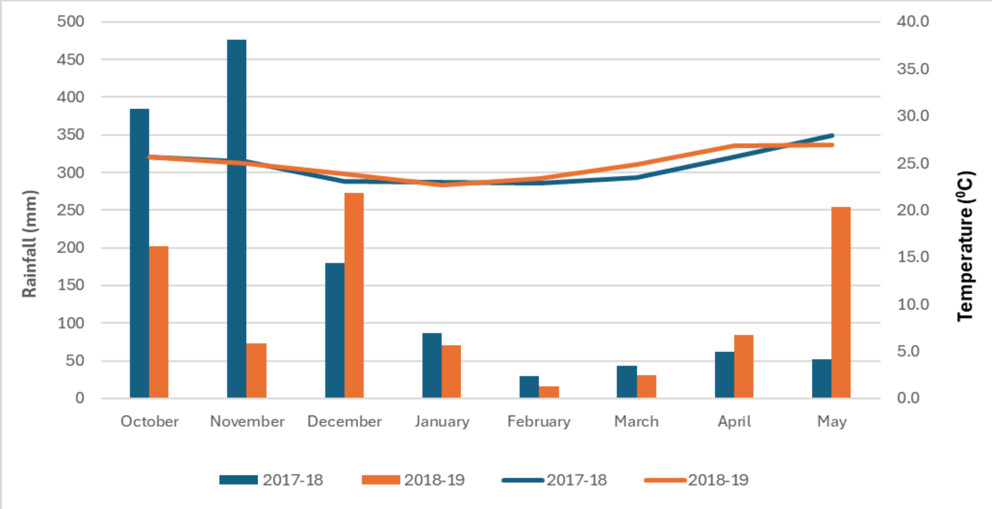

Figure 5.3. Monthly rainfall (CHIRPS) and temperature (ERA5) patterns comparing 2017–18 (normal year, left) and 2018–19 (drought year) dry seasons in northern Luzon

Table 5.1. Municipality-wise rice area estimated from CRISP rice maps from selected Municipalities in Cagayan Province, Luzon, Philippines during 2017-18 (normal) and 2018-19 (drought) dry seasons

Municipality	Province	CRISP estimated Rice Area (ha)		
		2017–18	2018–19	Area Change ha (%)
Abulug	Cagayan	4914	5051	137 (2.8%) ↑
Alcala	Cagayan	3725	4153	428 (11.5%) ↑
Allacapan	Cagayan	5867	5927	60 (1.0%) ↑
Amulung	Cagayan	7427	8253	826 (11.1%) ↑
Aparri	Cagayan	7864	10281	2417 (30.7%) ↑
Ballesteros	Cagayan	4457	4592	136 (3.0%) ↑
Buguey	Cagayan	4563	4637	74 (1.6%) ↑
Camalaniugan	Cagayan	4753	4715	-38 (-0.8%) ↓
Conner	Apayao	442	494	52 (11.8%) ↑
Enrile	Cagayan	2461	2787	327 (13.3%) ↑
Flora	Apayao	3087	3145	58 (1.9%) ↑
Iguig	Cagayan	903	1025	122 (13.5%) ↑
Lasam	Cagayan	6186	6324	139 (2.2%) ↑
Luna	Apayao	2063	2354	290 (14.1%) ↑
Pamplona	Cagayan	3554	3900	346 (9.7%) ↑
Piat	Cagayan	729	945	216 (29.6%) ↑
Pinukpuk	Kalinga	649	753	105 (16.2%) ↑
Pudtol	Apayao	758	1074	316 (41.7%) ↑
Rizal	Cagayan	202	268	66 (32.7%) ↑
Santa Marcela	Apayao	2835	2878	43 (1.5%) ↑
Santa Maria	Isabela	410	604	194 (47.3%) ↑
Santa Teresita	Cagayan	1941	2007	66 (3.4%) ↑
Santo Niño	Cagayan	1942	2142	200 (10.3%) ↑
Solana	Cagayan	11269	11882	613 (5.4%) ↑
Tuao	Cagayan	4647	5189	542 (11.7%) ↑
Tuguegarao City	Cagayan	666	976	310 (46.5%) ↑
Total		**88,312**	**96,359**	**8,047 (9.1%) ↑**

5.2.2. Rice Start-of-season

During the 2017-18 dry season, rice planting was concentrated almost entirely within the typical December–February window, accounting for nearly all the 88,312 ha cultivated that season (Table 5.2; Figure 5.5). January was the peak planting month, with 41,013 ha (46.4%), followed by 29,315 ha (33.2%) in December and 17,984 ha (20.4%) in February. No planting occurred outside this three-month window, indicating a highly synchronised and favourable establishment period, likely supported by timely irrigation release or adequate residual soil moisture. This narrow and uniform pattern suggests consistent planting behaviour across the region. In contrast, the 2018-19 dry season exhibited a more extended and irregular planting pattern across a total of 96,359 ha, likely influenced by delayed water availability and early-season drought conditions. Although January remained the dominant month with 58,871 ha (61.1%), December planting dropped sharply to 6,307 ha (6.5%), and February contributed 11,813 ha (12.3%). Planting continued well beyond the normal window, with substantial areas established in March (8,517 ha; 8.8%), and additional late planting in April (3,851 ha; 4.0%), May (1,620 ha; 1.7%), and June (933 ha; 1.0%). This extended distribution indicates that many farmers postponed planting, likely in response to delays in irrigation release and sporadic rainfall events.

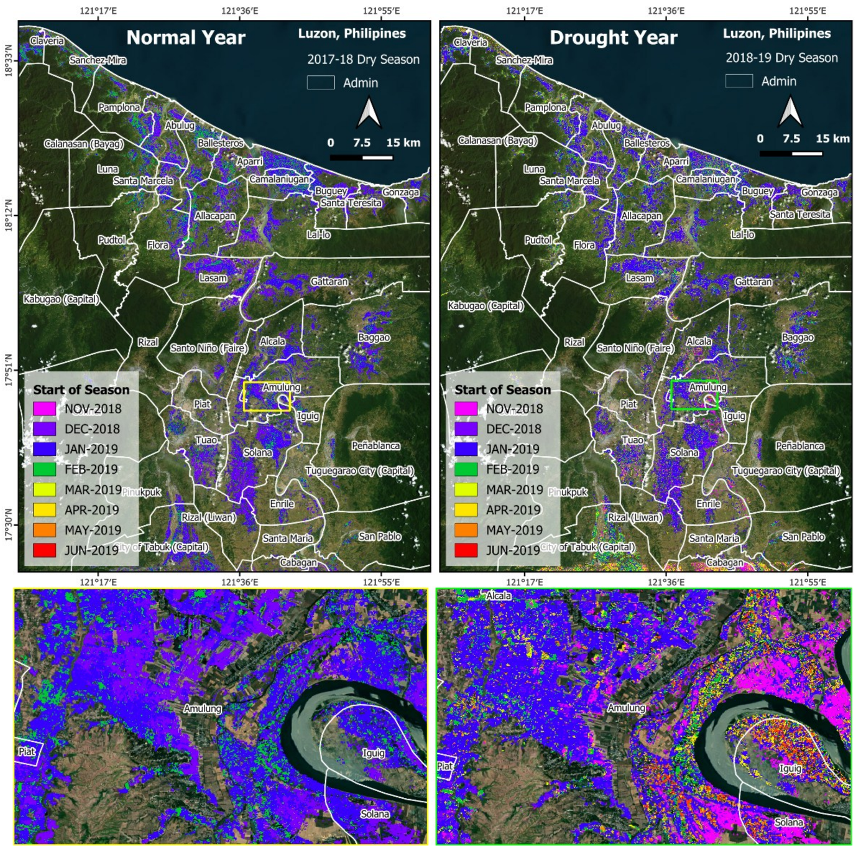

Figure 5.4. Start of Season wise rice area over the Cagayan Province in Luzon, Philippines, during the 2017–18 (normal year, left) and 2018–19 (drought year, right) dry seasons

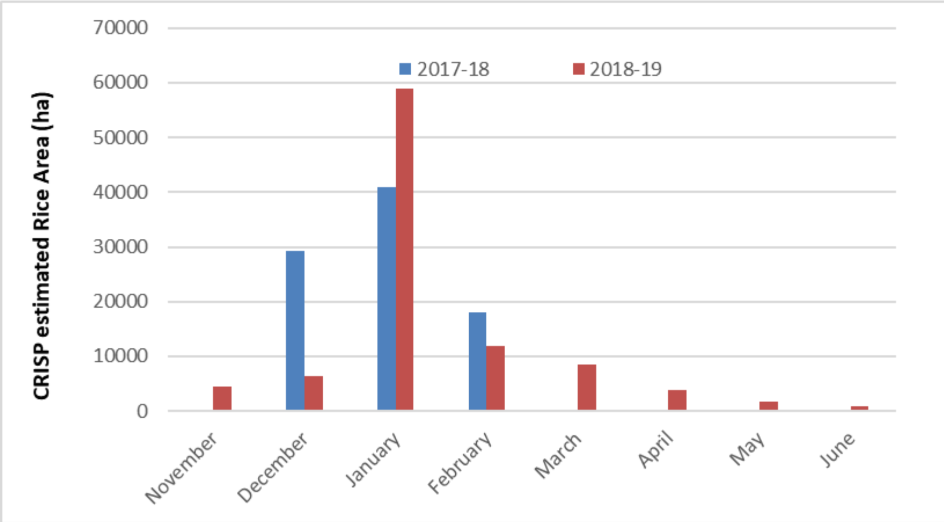

Figure 5.5. Comparison of month-wise rice planting area between the 2017–18 and 2018–19 dry seasons in selected Municipalities of Northern Luzon, Philippines

The monthly CRISP-estimated rice area patterns (Figure 5.5) reflect the contrasting rainfall conditions of the two seasons. In 2017-18, favourable early-season rainfall enabled timely field preparation and substantial December planting, leading to concentrated peaks in January and February. However, the 2018–19 season experienced severe rainfall deficits from October to December, sharply reducing December planting and pushing much of the field preparation into January. Farmers subsequently extended planting into March-June whenever water became available, either from short rainfall events or supplemental canal irrigation.

Table 5.2. Month-wise rice area (ha) by start of season (SoS) estimated from CRISP rice maps from selected Municipalities, Northern part of Luzon Province, Philippines, 2017-18 and 2018-19 dry season

Planted Month	Rice area planted month wise (ha)		
	2017–18 (Normal)	2018–19 (Drought)	Change in Planting (Drought)
November	0 (0)	4,282 (4.4)	4,282 (52.7%) ↑
December	29,255 (32.9)	6,259 (6.5)	–22,997 (–282.9%) ↓
January	41,090 (46.2)	59,303 (61.1)	18,213 (224.1%) ↑
February	18,563 (20.9)	11,973 (12.3)	–6,590 (–81.1%) ↓
March	0 (0)	8,803 (9.1)	8,803 (108.3%) ↑
April	0 (0)	3,842 (4.0)	3,842 (47.3%) ↑
May	0 (0)	1,656 (1.7)	1,656 (20.4%) ↑
June	0 (0)	920 (0.9)	920 (11.3%) ↑
Total	88,909	97,037	8,128 ↑

5.2.3. Rice Yield

A comparison of rice yields between the 2017–18 and 2018–19 seasons shows a consistent decrease across all municipalities. In 2017–18, yields averaged 4.2 t/ha, but this dropped to 3.23 t/ha in 2018–19 with an average reduction of nearly 950 kg/ha. Every municipality recorded lower yields in the second season, with decreases generally ranging from -300 to over -1,400 kg/ha. The percentage decline also varied widely. Municipalities such as Aparri, Buguey, Lasam, and Santa Teresita showed reductions of 6-16%, while the most severely affected ones including Abulug, Flora, Solana, Alcala, and Luna, experienced losses exceeding 30-36%. This uniform pattern of decline indicates that the factor affecting yield was broad, widespread, and external rather than municipality specific.

This substantial drop in productivity can be attributed largely to the prolonged dry spell experienced during the 2018–19 cropping season. Rice is highly sensitive to water stress, especially during its critical growth stages, and insufficient moisture can significantly reduce tiller formation, hamper nutrient uptake, and limit grain filling. With reduced rainfall and more limited irrigation water during the dry spell, fields were likely unable to maintain optimal growing conditions, leading to stunted plant growth and ultimately lower yields. The consistency of the decline across municipalities highlights how the dry spell acted as a region-wide environmental stressor, underscoring the vulnerability of rainfed and poorly irrigated rice areas to extended periods of drought.

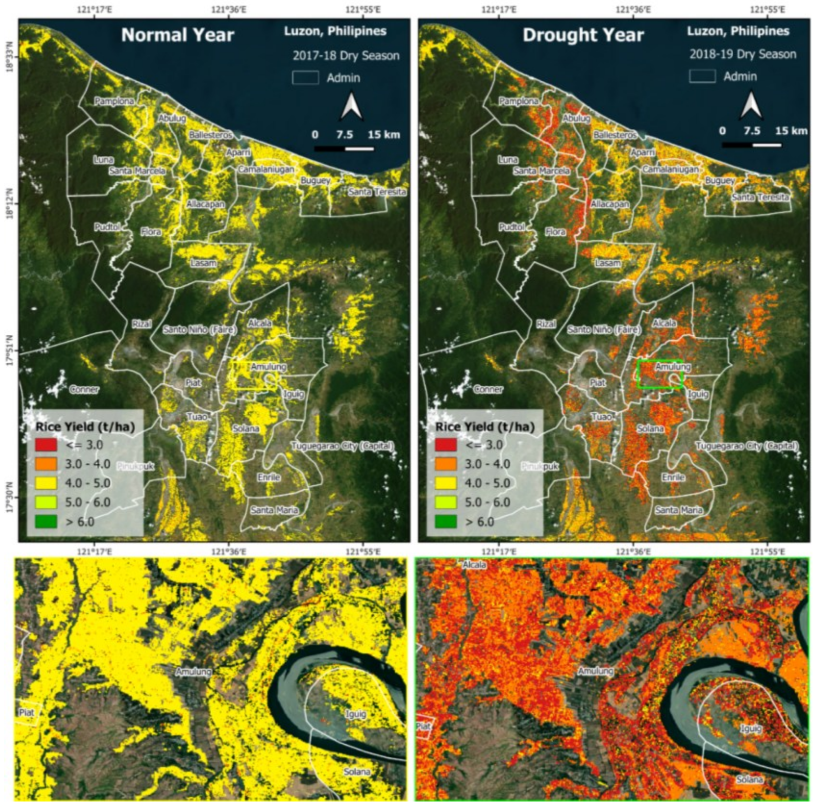

Figure 5.5. Rice yield over the Cagayan Province in Luzon, Philippines during the 2017–18 (reference, left) and 2018-19 (drought, centre) dry seasons, and the corresponding yield reduction due to drought (right).

Table 5.3. Municipality-wise CRISP rice yield (kg/ha) from selected Municipalities from the Northern part of Luzon province, Philippines during the 2017-18 and 2018-19 dry seasons and changes

Municipality	Rice yield in (Kg/ha) and change in the yield (%)		
	2017–18	2018–19	Change in yield
Abulug	4158	2676	–1482 (–35.6%) ↓
Alcala	4181	2902	–1279 (–30.6%) ↓
Allacapan	4198	3532	–666 (–15.9%) ↓
Amulung	4179	2857	–1322 (–31.6%) ↓
Aparri	4180	3892	–288 (–6.9%) ↓
Ballesteros	4172	3500	–672 (–16.1%) ↓
Buguey	4184	3813	–371 (–8.9%) ↓
Camalaniugan	4165	3761	–404 (–9.7%) ↓

Conner	4131	3542	–589 (–14.3%) ↓
Enrile	4181	2998	–1183 (–28.3%) ↓
Flora	4181	2688	–1493 (–35.7%) ↓
Iguig	4172	3113	–1059 (–25.4%) ↓
Lasam	4208	3782	–426 (–10.1%) ↓
Luna	4196	2918	–1278 (–30.5%) ↓
Pamplona	4147	2983	–1164 (–28.1%) ↓
Piat	4163	3145	–1018 (–24.5%) ↓
Pudtol	4195	3245	–950 (–22.7%) ↓
Rizal	4212	3286	–926 (–22.0%) ↓
Sanchez-Mira	4116	3404	–712 (–17.3%) ↓
Santa Marcela	4164	2993	–1171 (–28.1%) ↓
Santa Maria	4149	3109	–1040 (–25.1%) ↓
Santa Teresita	4213	3852	–361 (–8.6%) ↓
Santo Niño (Faire)	4216	3188	–1028 (–24.4%) ↓
Solana	4197	2843	–1354 (–32.3%) ↓
Tuao	4161	2983	–1178 (–28.3%) ↓
Tuguegarao City	4171	2928	–1243 (–29.8%) ↓
Total	**4177**	**3228**	–949 (–22.7%) ↓

5.3. Data used for CRISP products validation

For the Luzon site, a total of 33 rice field validation points were available for assessing the accuracy of the CRISP-derived rice area map for the 2018-19 dry season (Figure 5.6). No non-rice field validation was available, so 40 non-rice points were systematically identified and collected using high-resolution Google Earth imagery, focusing only on permanent non-rice land cover types, such as shrubland, grassland, perennial plantations, and marshland. All validation points were used as independent reference data and were not involved in the calibration or generation of the CRISP rice map for Luzon. No validation data were available for the 2017-18 dry season. For yield validation, only province-level rice yield statistics published by the Philippine Statistics Authority (PSA) were used as the reference dataset for both the 2017–18 and 2018–19 dry seasons, as no field-based crop cut or farmer-reported yield data were available for the Luzon site. The PSA data used to be derived from quarterly Palay Production Surveys (PPS) where trained enumerators collect farmer-reported data on harvested area and production from a statistically selected sample of households. These data are only available at Province level.

5.4. Results of CRISP products validation

5.4.1. Rice area

A confusion matrix was used to evaluate the accuracy of the CRISP-derived rice map for the 2018-19 dry season in selected municipalities of Cagayan Province in Luzon, Philippines. The map achieved an overall accuracy of 84.9% with a Kappa index of 0.70, indicating good agreement between the predicted rice extent and the reference validation points (Table 5.4). Class-wise, rice fields were mapped with an accuracy of 72.7%, reflecting moderate omission errors, while non-rice areas were classified with a much higher accuracy of 95.0%, demonstrating that the model was more effective in excluding non-rice land covers than detecting rice. Reliability values showed a similar pattern, with 92.3% reliability for rice (i.e., most pixels labelled as rice were correct) and 80.9% reliability for non-rice, resulting in an average reliability of 86.6%. The relatively lower rice detection accuracy was mainly due to the omission of some actual rice fields, particularly small, fragmented, and likely influenced by mixed-pixel effects and weaker temporal signatures during the dry season. Overall, the validation indicates that the CRISP product provided a reliable representation of rice distribution during the season, with strong performance for non-rice discrimination and moderate underestimation of rice areas.

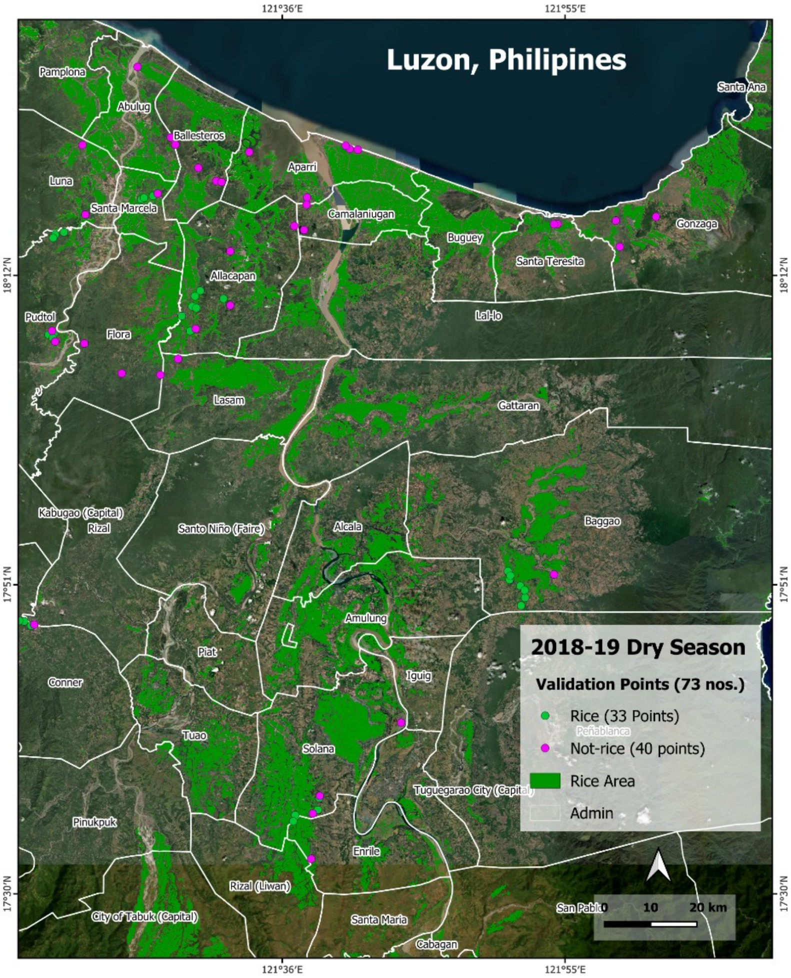

Figure 5.6. Spatial distribution of validation points (rice and non-rice) used for the 2028-19 Dry Season CRISP rice map validation over the Cagayan Province in Luzon, Philippines

Table 5.4. Confusion matrix for the rice area classification from selected Municipalities from the Northern part of Luzon province, during the 2018-19 dry season

CRISP Rice map: 2018-19 Dry Season				
Predicted class from the map				
		Rice	**Non-rice**	**Accuracy**
Actual class (survey)	**Rice**	24	9	72.7%
	Non-rice	2	38	95.0%
	Reliability	92.3%	80.9%	84.9%
Average accuracy		83.9%		
Average reliability		86.6%		
Overall accuracy		**84.9%**		
Kappa index		0.70		

5.4.2. Rice yield

The CRISP-derived rice yield estimates were compared to province-level yield data from the Philippine Statistics Authority (PSA). Hence no yield reference spatial data were available at all. The PSA data come from ground-based surveys, farmer reports, and administrative records, which typically reflect actual harvest outcomes but may have their own uncertainties related to sampling, reporting accuracy, and data aggregation at the provincial level.

For the 2017-18 dry season in Cagayan Province, CRISP predicted an average yield of 4.18 t/ha, while PSA reported 4.76 t/ha, resulting in an underestimation yield, a RMSE of 0.58 t/ha and a NRMSE of 14%, indicating moderate accuracy. Model performance appeared to decline significantly in the 2018–2019 dry season, where CRISP estimated only 3.23 t/ha against the PSA yield of 4.34 t/ha. This larger discrepancy yielded an RMSE of 1.11 t/ha and an NRMSE of 34%. During this year, widespread drought (prolonged dry spell associated with El Nino phenomenon) affected the whole country with severe impact in Cagayan province. Both approaches detected a reduction of yield linked to the drought, with a yield reduction 8.8% and 22.7%, for the PSA data, and the CRISP data, respectively.

Season	**Province**	**Average CRISP estimates (t/ha)**	**PSA data (t/ha)**	**RMSE (t/ha)**	**NRMSE (%)**
2017-2018 DS	Cagayan	4.18	4.76	0.58	14
2018-2019 DS	Cagayan	3.23	4.34	1.11	34

6. Validation of the Senegal River Valley, Senegal site

6.1. Site

Senegal is located on the west coast of Africa and shares borders with Mauritania, Mali, Guinea, and Guinea-Bissau. It lies within the Sahel region, a transition between the Sudanian savannas and the Sahara. Since the 80s, rice demand has surpassed those of more traditional crops such as sorghum and millet, and the country imports 70% of its national rice consumption (957,000 tons in 2019). The Senegal River Valley (SRV) is a large river basin that drains 270,000 km^2 of land from Mali, Senegal, and Mauritania (Figure 6.1). Irrigated rice is dominant in the Senegal River Valley, which accounts for almost 70% of Senegal rice production, while the remaining production comes from rainfed rice cultivation in Central Senegal and in the Casamance region. Annual rainfall in SRV is about 400 mm (e.g., Louga and St. Louis), making rainfed agriculture challenging. The valley hosts 240,000 ha of irrigated production systems, allowing cultivation in the rainy season (July–December) and hot dry season (February–July). Recently, a shift from single wet season cropping to dry season rice cropping or double cropping, has been observed to capitalize on higher yields in the dry season. Average yield is between 5 to 6 tons/ha, generally on average farms varying between 0.25 and 2 ha. Production is mechanized with access to tractors, harvesters, or other farm equipment. In irrigated lands the main challenges relate to salinity, bird and pest attacks, and spells of low temperature, while improper weed and fertilizer management or late sowing/harvesting also contribute to yield gaps.

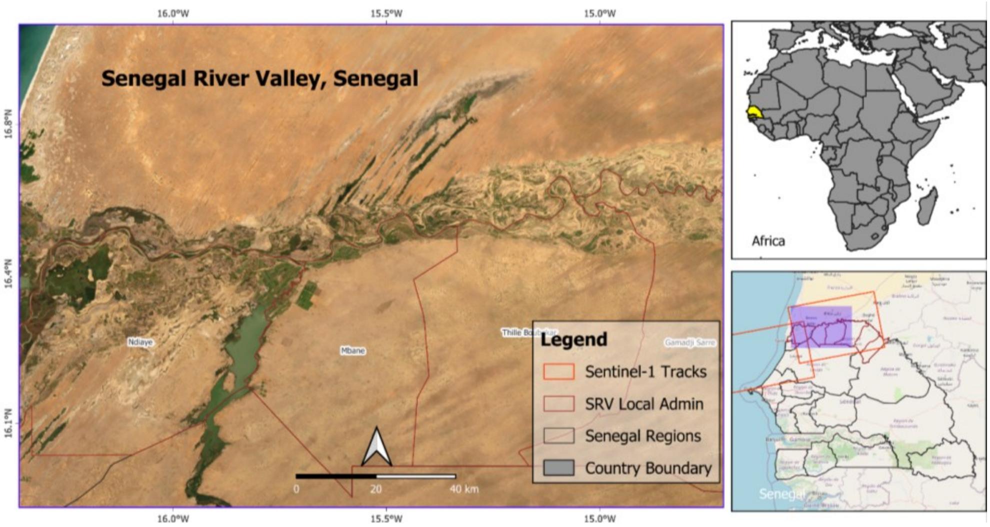

Figure 6.1. The Senegal River Valley site, Senegal

6.2. Rice CRISP products

As part of the CRISP standard algorithm, three rice products were generated for the SRV site: RA, SoS, and yield for the 2023 wet season (July-December) (see Figures 6.2-6.4).

6.1.1. Rice Area

Overall, the rice area map (Figure 6.2) shows that wet season rice cultivation is predominantly concentrated in the delta region of the Dagana Department, consistent with earlier studies (Tanaka et al., 2015; Busetto et al., 2019; Mane et al., 2024). The total rice area derived from the CRISP map was 28,766 ha (Table 6.1). Within Dagana, Ndaye Arrondissement accounted for the largest rice area of 16,589 ha, followed by Mbane (4,049 ha). In Podor, the Thille Boubakar, Cas-Cas, Gamadji Sarre, and Salde Arrondissements recorded lower rice area compared to Dagana Department Arrondissements. Overall, Dagana accounted for a major proportion of the rice area in the Senegal River Valley (SRV), indicating intensive cultivation in the Dagana delta tract, while the Podor contributed smaller but spatially contiguous rice clusters.

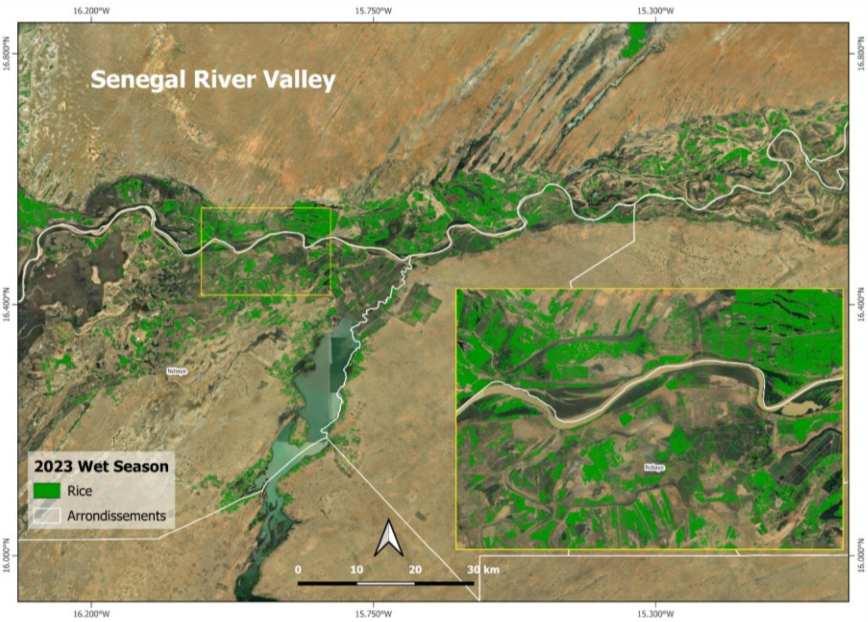

Figure 6.2. Spatial distribution of rice area in the Senegal River Valley derived from CRISP rice maps, 2023 wet season

Table 6.1. Arrondissement-wise rice area (ha) by start of season (SoS) month and rice yield estimated from CRISP rice maps from Dagana and Podor Departments, Senegal River Valley, 2023 wet season

Arrondissement (Department)	SoS date-wise Rice Area, ha (%)				Rice Yield (t/ha)
	Jul	Aug	Sep	Total	
Mbane (Dagana)	1,236 (30.5)	1,113 (27.5)	1,700 (42.0)	4,049	4.15
Ndiaye (Dagana)	3,574 (21.5)	6,680 (40.3)	6,336 (38.2)	16,589	4.6
Thille Boubakar (Podor)	718 (36.9)	443 (22.8)	783 (40.3)	1,944	4.3
Cas-Cas (Podor)	1,574 (54.3)	671 (23.2)	651 (22.5)	2,896	4.1
Salde (Podor)	212 (47.4)	188 (42.1)	47 (10.5)	447	3.6
Gamadji Sarre (Podor)	1,138 (40.0)	786 (27.6)	917 (32.3)	2,841	4.8
Total	**8,453 (29.4)**	**9,880 (34.3)**	**10,433 (36.3)**	**28,766**	**4.3**

6.1.2. Start-of-Season (SoS)

The Start-of-Season (SoS) estimates derived from the CRISP-generated map reveal distinct spatial and temporal variations in rice planting across the SRV (Figure 6.2). Overall, July planting covered 8,453 ha (29.4%), August accounted for the largest share with 9,880 ha (34.3%), and September contributed 10,433 ha (36.3%) (Table 6.1). The dominance of August and September plantings reflects a staggered and extended transplanting window, coinciding with the peak of the wet season when rainfall and irrigation water availability are at their highest. This period represents the most favourable conditions for field preparation and transplanting across most parts of the valley (Gebremichael et al., 2022). Early planting in July occurred primarily in areas with reliable water access, such as those close to main irrigation canals or equipped with controlled water management systems. Farmers in these areas take advantage of early dam water releases to establish crops sooner, enabling earlier harvests and facilitating subsequent dry-season cultivation (e.g., vegetables or a second rice crop) (Le Gal and Papy, 1998; Van Oort et al., 2016; Dingkuhn, 1995). This temporal pattern aligns with the operational phases of irrigation releases and farmers' access to water along the canal system.

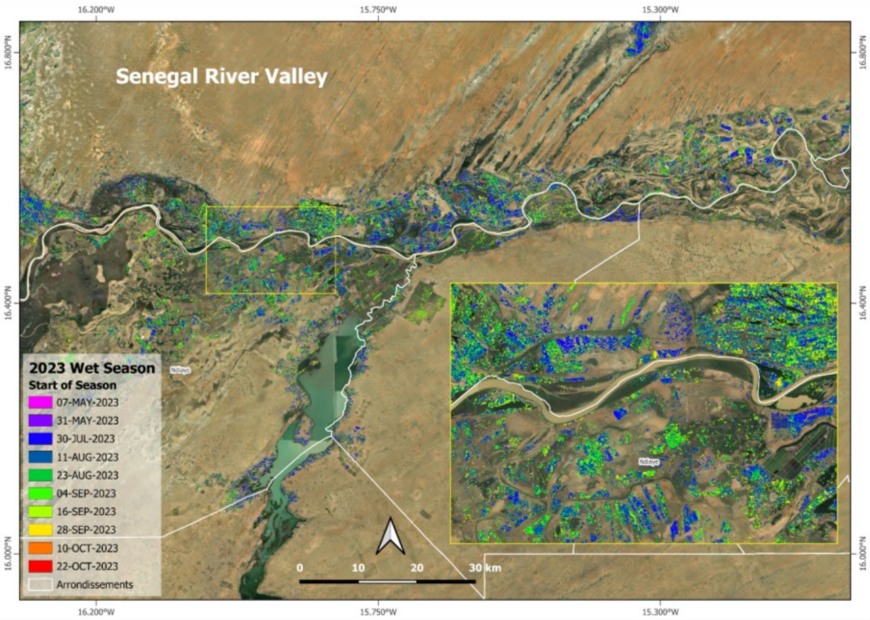

Figure 6.3. Start-of-Season (SoS) rice planting distribution in the Senegal River Valley (SRV) derived from CRISP rice maps for the 2023 wet season

6.1.3. Rice Yield

The rice yield map estimates (Figure 6.4) indicated an average yield of 4.1 t/ha across the valley, including Dagana and Podor Departments (Table 6.1). The highest average yield was observed in Gamadji Sarre (4.6 t/ha), followed by Ndiaye (4.4 t/ha), Thille Boubakar (4.3 t/ha) and Cas-Cas/Mbane (4.1 t/ha). On the other hand, Salde reported the lowest average yield (3.6 t/ha). The observed spatial variability in yield likely reflects differences in irrigation reliability and crop management practices rather than planting period alone. Higher yields in the delta zones of Dagana (e.g., Ndiaye) and central Podor (e.g., Gamadji Sarre) can be linked to well-maintained irrigation infrastructure, consistent and timely water supply, and generally better crop management. In contrast, areas such as Salde, located in the northernmost part of Podor, may experience limited irrigation efficiency and poor crop management practices, including inconsistent access to high-quality seeds. Furthermore, late planting in some locations can coincide with the arrival of migratory birds from Europe during the crop maturation stage, resulting in significant yield losses due to bird damage (OMVS and IRD, 2002; Tanaka et al., 2015).

6.3. Data used for CRISP products validation

A total of 195 field-visited points were geo-tagged during the 2023 wet rice growing season (July-September), consisting of 101 rice and 94 non-rice fields (Figure 6.5). For non-rice points, the focus was mainly on seasonal crop fields such as maize, onion, and tomato, which are the main potential source of errors with rice crops. A few points were also collected for other land covers, easily distinguished from rice crops, such as fallow land and shrubland. Field data were collected by the Institut Sénégalais de Recherche Agricole (ISAR) and used to assess the accuracy of the CRISP-generated rice map. These were independent from the calibration points used for CRISP rice map generation. In addition to these datasets, 15 yield data points or crop cut experiments (CCEs) were available across the valley. However, only 8 points could be used as the remaining data were found to have quality issues. These CCEs served as independent references to assess the CRISP-derived rice yield map for the 2023 wet season.

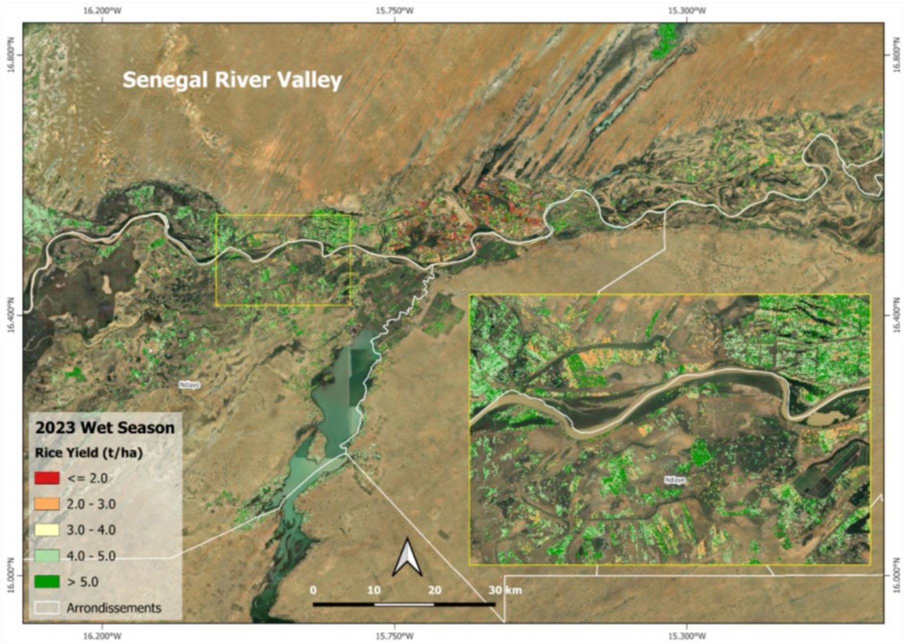

Figure 6.4. Spatial distribution of rice yield (t/ha) in the Senegal River Valley derived from CRISP rice maps, 2023 wet season

6.4. Results of CRISP products validation

6.4.1. Rice area

A confusion matrix was used to validate the CRISP rice area map. The overall accuracy was 81.5% with a Kappa index of 0.63, reflecting a good agreement between the rice area classification and field observations (Table 6.2). Class-wise assessment showed that rice fields were detected with 85.1% accuracy, while non-rice areas were better classified at 87.2%, suggesting that CRISP outputs tend to slightly underestimate rice areas and occasionally misclassify some non-rice fields as rice. The map captured most of the rice fields across the valley; however, scattered pixels were misclassified as non-rice within otherwise homogeneous rice zones, and field boundaries near other land covers were often omitted. These scattered omission errors contributed to a salt-and-pepper effect and reduced rice classification accuracy, resulting in the omission of 23.8% of actual rice pixels. This may result from shortcoming on the SAR data processing, possibly in relation with the image temporal filtering. The few commission errors, where non-rice areas were misclassified as rice, primarily occurred in rice fallow lands with grass cover that emerged after early-season rain, producing a SAR temporal signature similar to wet-season rice fields.

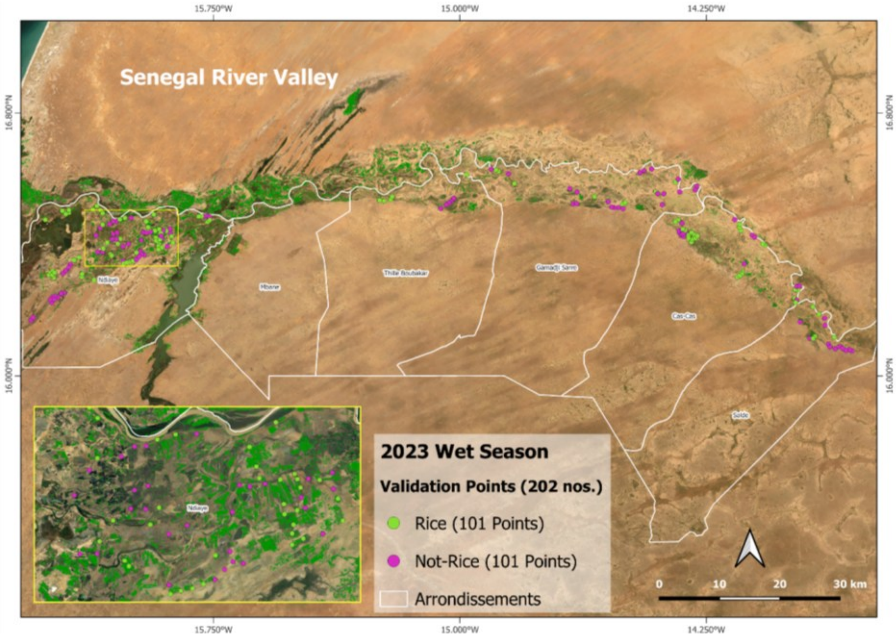

Figure 6.5. Spatial distribution of validation points (rice and non-rice) used for the CRISP rice map validation in the Senegal River Valley, 2023 wet season

In addition, we compared the CRISP rice map with the continental rice area map (Africa 20 m) produced by Jiang et al. (2025). This comparison involved both accuracy assessment and spatial overlap analysis. The Africa 20m map achieved an overall accuracy of 59.5% and a kappa index of 0.19, indicating only fair agreement with ground validation data. CRISP provided a more accurate and reliable classification of rice areas, particularly in excluding non-rice land cover (Table 6.2). In the Africa 20m map, vegetable crops such as tomato and onion and sugarcane plantations, which grow during the same period as wet-season rice, were often misclassified as rice. In addition, although CRISP also showed slight commission of rice fallow fields, the Africa 20 m map committed a larger portion of rice fallow fields with grass growth as rice, according to the validation data.

Approximately 15,500 ha (19.3%) of rice area was consistently captured in both products (Table 6.3). However, the Africa 20m map reported a much larger unique rice extent (52,000 ha; 64.7%), while CRISP identified only about 13,000 ha (16%) as unique rice area. The Africa 20m product, therefore, likely overestimates rice extent, as reflected in the significant inclusion of non-rice samples within the rice class (59.5% accuracy). Spatial overlap was highest in Cas-Cas and Salde (>65%), suggesting good consistency in these locations. Overall, while the Africa 20m product provides broader continental coverage, it suffers from higher commission errors arising from spectral confusion with other irrigated crops and might be limited by insufficient calibration ground data for rice classification, whereas CRISP offers more accurate non-rice discrimination and greater consistency in rice mapping at local scales.

Table 6.2. Confusion matrix for the rice area classification produced at the African continental level by Jiang et al. (2025) for the wet season of 2023, and in the Senegal River Valley (SRV). Validation used the same 2023 field-collected points discussed in section 6.3.

CRISP Rice map					**Africa 20M Rice map (Jiang et al., 2025)**				
Predicted class from the map					Predicted class from the map				
		Rice	**Non-rice**	**Accuracy**			**Rice**	**Non-rice**	**Accuracy**
	Rice	77	24	76.2%		**Rice**	69	32	68.3%

Actual class (survey)	**Non-rice**	12	82	87.2%	Actual class (survey)	**Non-rice**	47	47	50.0%
	Reliability	86.5%	77.4%	**81.5%**		**Reliability**	59.5%	59.5%	**59.5%**
Average accuracy		81.7%			Average accuracy		59.2%		
Average reliability		81.9%			Average reliability		59.5%		
Overall accuracy		**81.5%**					**59.5%**		
Kappa index		0.63			Kappa index		0.19		

Table 6.3. Arrondissement-wise comparison of rice area mapped by the CRISP rice map and the Africa 20 m rice map (Jiang et al., 2025), 2023 wet season, Dagana and Podor Departments, Senegal River Valley

Arrondissement (Department)	Rice Area in ha			
	Only CRISP	**Only Africa 20m**	**Both**	**Total**
Mbane (Dagana)	1747 (18.3)	6180 (64.7)	1631 (17.1)	9557
Ndiaye (Dagana)	9082 (17.1)	36806 (69.5)	7092 (13.4)	52980
Thille Boubakar (Podor)	992 (14.4)	4803 (69.9)	1077 (15.7)	6872
Cas-Cas (Podor)	464 (10.8)	962 (22.3)	2879 (66.9)	4305
Salde (Podor)	71 (6.9)	209 (20.4)	743 (72.6)	1023
Gamadji Sarre (Podor)	501 (9.0)	3023 (54.1)	2066 (37.0)	5590
Total (Dagana & Podor)	12857 (16.0)	51982 (64.7)	15488 (19.3)	80327

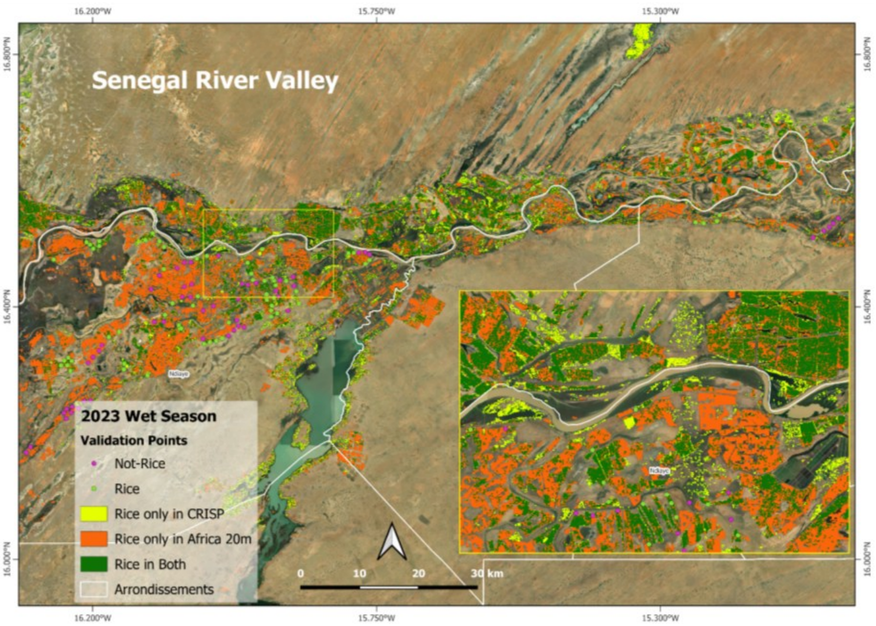

Figure 6.6. Comparison of the CRISP rice area map and rice area map produced at the African continental level by Jiang et al. (2025) for the wet season of 2023

6.4.2. Rice yield

Table 6.4 compares CRISP yield estimates with Crop Cutting Experiment (CCE) yields across four arrondissements in the Dagana and Podor departments. CCEs are field sampling method used to estimate crop yield by harvesting and weighting a small randomly selected portion of a field. Overall, the CRISP model shows moderate accuracy, with an average predicted yield of 4.14 t/ha compared to an actual CCE yield of 4.03 t/ha. The overall RMSE of 0.11 t/ha and NRMSE of 2.7% indicate that the model performs well but with some variation across locations. Ndiaye shows the highest discrepancy, with an NRMSE of 20%, suggesting that CRISP significantly underestimates yield there, while Mbane demonstrates excellent accuracy with a very small NRMSE error of 1.8%. Thille Boubakar and Cas-Cas show moderate error levels, with NRMSE values of 15% and 16%, respectively. However, the number of CCE fields used for comparison is very small—only 8 in total, with some arrondissements represented by a single field—which limits the reliability of the conclusions. Because of this low and uneven sample size, the accuracy results should be interpreted cautiously, as the CCE yields may not fully represent the true yield variability in each area.

Table 6.4. Comparison of yield estimates with CCEs in the Senegal River Valley, 2023 wet season

Arrondissement (Department)	No. of CCE fields	Average CRISP estimates (t/ha)	CCE yield (t/ha)	RMSE (t/ha)	NRMSE (%)
Ndiaye (Dagana)	3	4.43	5.33	0.90	20
Mbane (Dagana)	1	3.98	3.91	0.07	1.8
Thille Boubakar (Podor)	1	4.13	3.51	0.62	15
Cas-Cas (Podor)	3	4.03	3.37	0.66	16
TOTAL	**8**	**4.14**	**4.03**	**0.11**	**2.7**

7. Validation of the Kano, Nigeria site

7.1. Site

Nigeria is the largest rice producer in Africa, followed by Egypt, Madagascar, and Tanzania, with an estimated 8.9 million metric tons of paddy rice produced in 2023. Despite of this, the country still relies on significant imports to meet its domestic demand. The Kano State is in northern Nigeria (Figure 7.1), a semi-arid region with both rainfed and irrigated rice cultivation. In rainfed areas small-scale and low-yield wet season rice farming concerns most of the farmers. Rice cultivation in irrigated areas is concentrated within major projects such as the Kano River Irrigation Project and the Hadejia Valley Project. Irrigation schemes provide controlled water supply that allows cultivation in both wet and dry seasons, flexible planting times, effective use of inputs, and higher yields than rainfed smallholder farms. The landscape is characterised by a flat topography. During the wet season, rice is typically planted between May and August, whereas during the dry season transplanting occurs mainly from February to March. Inter-annual rainfall variability, however, can shift these dates, particularly in rainfed systems.

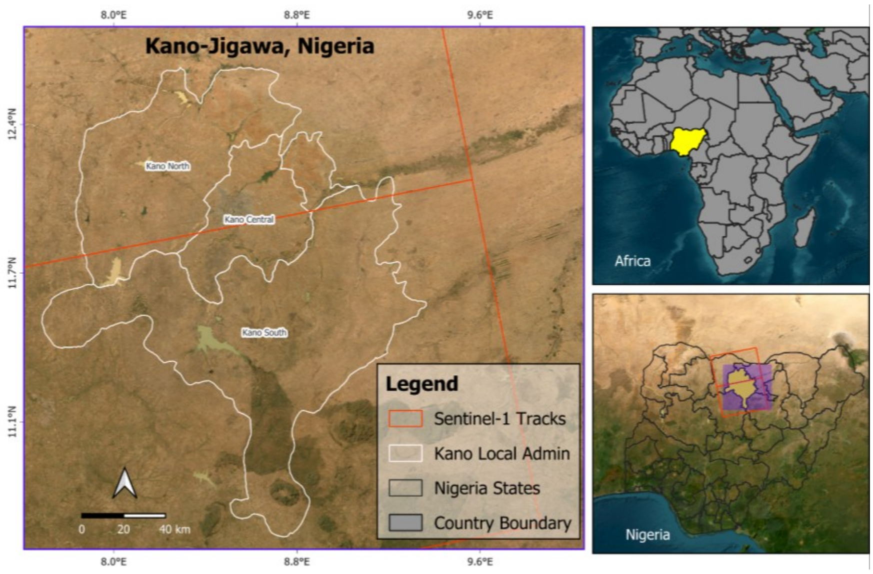

Figure 7.1. Kano-Jigawa site, Nigeria

7.2. Rice CRISP products

For the Kano, the CRISP standard algorithm was applied separately to the irrigated and rainfed RIICE ecosystems. These ecosystems exhibit distinct responses in satellite observations, and different classification parameters were optimised for each. For both ecosystems, three rice products were generated for the 2023 wet season (July–December): RA, SoS and yield. The outputs from irrigated and rainfed maps were subsequently mosaicked to produce consistent maps for the Kano site. Rainfed upland rice is marginal in the northern Nigerian states and was not considered specifically in the rice mapping. Figures 7.2-7.4 present these products.

7.2.1. Rice Area

The rice area map (Figure 7.2) shows the wet season rice cultivation distribution in the Kano State of Nigeria. The total rice area for Kano State during the 2023 wet season was estimated at 206,139 ha. The rice area was mainly dominated by rainfed lowland ecosystems, which accounted for 187,553 ha (Table 7.1). This represented more than 90% of the total rice extent, pretty much scattered across the whole state, with higher rice area in Kano west and south-west. In contrast, irrigated rice covers a much smaller area with 18,586 ha (9%), distributed in a few large government-managed irrigation schemes. Across senatorial districts, Kano South reported the largest rainfed rice extent (104,412 ha), followed by Kano North (60,616 ha) and Kano Central (22,525 ha). For irrigated rice, Kano Central contributed the largest share (11,009 ha), with smaller areas observed in Kano South (3,839 ha) and Kano North (3,738 ha).

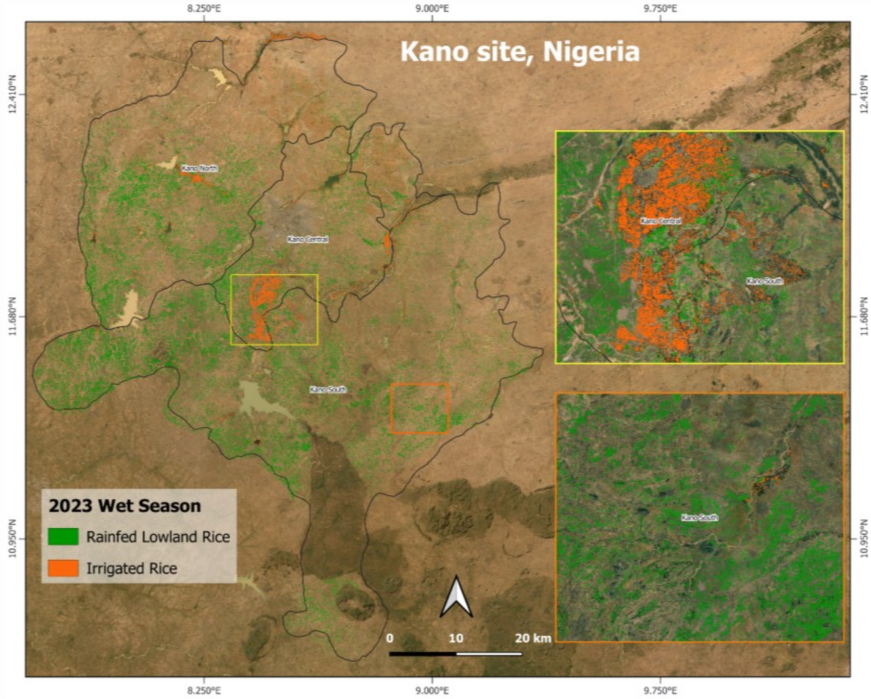

Figure 7.2. Spatial distribution of CRISP rice area in the Kano State, Nigeria, 2023 wet season

7.2.3. Rice Start-of-Season (SoS)

The planting/sowing dates (Figure 7.3) show distinct temporal patterns according to rice ecosystems. In rainfed lowlands, planting took place predominantly in June (106,739 ha, 57%) and July (76,589 ha, 41%), aligning closely with the onset of the wet season rainfall. Earlier/later planting was marginal and only contributed around 2% of the total rainfed rice. The irrigated schemes exhibited a more distributed planting pattern over the season, with later major sowings in July (8,512 ha, 46%), and August (7,343 ha, 40%) and smaller but notable areas sown in June or September. This extended planting window reflects the capacity of irrigation schemes to buffer against rainfall variability and to support "off-peak" planting.

Table 7.1. Rice area by Start of Season (SoS) and rice yield in Kano State, Nigeria, 2023 Wet Season

Senatorial District	SoS wise rice area (ha, in bracket are % area)								Rice Yield (t/ha)
	May	Jun	Jul	Aug	Sep	Oct	Nov	Total	
Rainfed Lowland Region									
Kano South	64 (0.1)	62585 (59.9)	38194 (36.6)	3566 (3.4)	-	-	4 (0.0)	104412	3.50
Kano Central	14 (0.1)	16014 (71.1)	6364 (28.3)	127 (0.6)	-	-	6 (0.0)	22525	3.47

Kano North	5 (0.0)	28140 (46.4)	32030 (52.8)	439 (0.7)	-	-	2 (0.0)	60616	3.47
Irrigated Region									
Kano South	-	367 (9.6)	2324 (60.5)	919 (23.9)	184 (4.8)	40 (1.0)	5 (0.1)	3839	4.81
Kano Central	-	352 (3.2)	2795 (25.4)	6849 (62.2)	958 (8.7)	48 (0.4)	8 (0.1)	11009	4.93
Kano North	-	117 (3.1)	1804 (48.3)	1536 (41.1)	253 (6.8)	26 (0.7)	3 (0.1)	3738	4.82
Kano State Total	82 (0.0)	107575 (52.2)	83512 (40.5)	13435 (6.5)	1395 (0.7)	114 (0.1)	27 (0.0)	**206139**	**4.17**

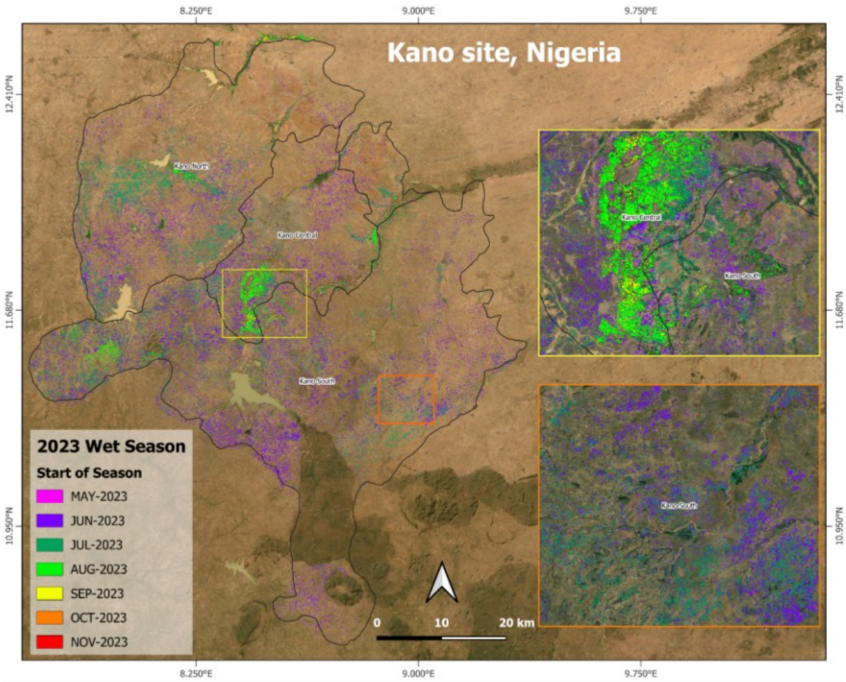

Figure 7.3. Start of season (SoS) rice planting distribution in the Kano site, Nigeria, derived from CRISP rice maps for the 2023 wet season

7.2.4. Rice Yield

As expected, yield estimates (Figure 7.4) revealed a clear contrast between rainfed lowland and irrigated rice ecosystems. Rainfed lowland rice reported an average productivity of 3.5 t/ha across districts. This is likely caused by the low-input, smallholder rice farm holdings, and the dominance of subsistence to semi-commercial of rice farming systems in the region. By comparison, irrigated rice achieved substantially higher yields, averaging 4.8 t/ha. The higher yield in irrigated rice fields may reflect better water control, crop management, and/or access to better seeds, that increase the productivity in semi-arid northern Nigeria. These results emphasise both the vulnerability of rainfed rice systems to rainfall variability and the strategic importance of irrigation in meeting growing rice demand.

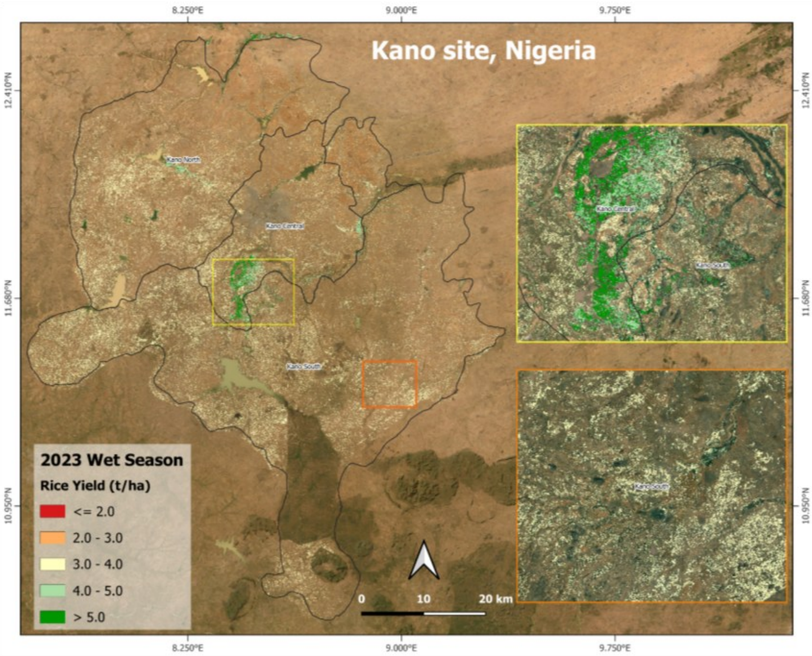

Figure 7.4. Spatial distribution of CRISP rice yield (t/ha) for Kano State, Nigeria, 2023 wet season

7.3. Data used for CRISP products validation

A total of 246 field-visited points were geo-tagged during the 2023 wet rice growing season (July–September) across the Kano site, Nigeria (Figure 7.5). These consisted of 153 rice and 93 non-rice fields. The rice observations included both irrigated and rainfed lowland systems, which represent the major rice cultivation practices in the region. The non-rice samples covered a range of important seasonal crops such as millet, sorghum, maize, sugarcane, and cassava, which are the primary sources of potential confusion with rice. Field data collection was undertaken by a local Africa Rice team. The validation points were independent of the calibration dataset used in the CRISP rice mapping process. For the yield validation, farmer's actual yield data also collected by a local Africa Rice team were used. A total of 192 and 158 farmer's actual yield data under the irrigated and rainfed areas, respectively, were used in the validation exercise.

7.4. Results of CRISP products validation

7.4.1. Rice area

The CRISP Rice Area product yielded an overall accuracy of 81.2% and a Kappa index of 0.62, indicating a moderate agreement with field data (Table 7.2). Class-wise evaluation showed that rice fields were mapped with 79.5% accuracy, while non-rice areas were mapped with 84.0% accuracy. Reliability assessment indicated that predicted rice pixels had a high likelihood of being true rice (88.9%), meaning they were correctly classified as rice in most cases, whereas predicted non-rice pixels had a reliability of 71.8%. These results proved to be more effective in identifying non-rice areas, while some rice fields could be omitted, particularly in rainfed regions, leading to omission errors in the Non-Rice category, and a possible underestimation of rice areas. The omission of rice pixels may be attributed to some spectral and spatial mixing at field boundaries or confusion with other vegetation types during the season.

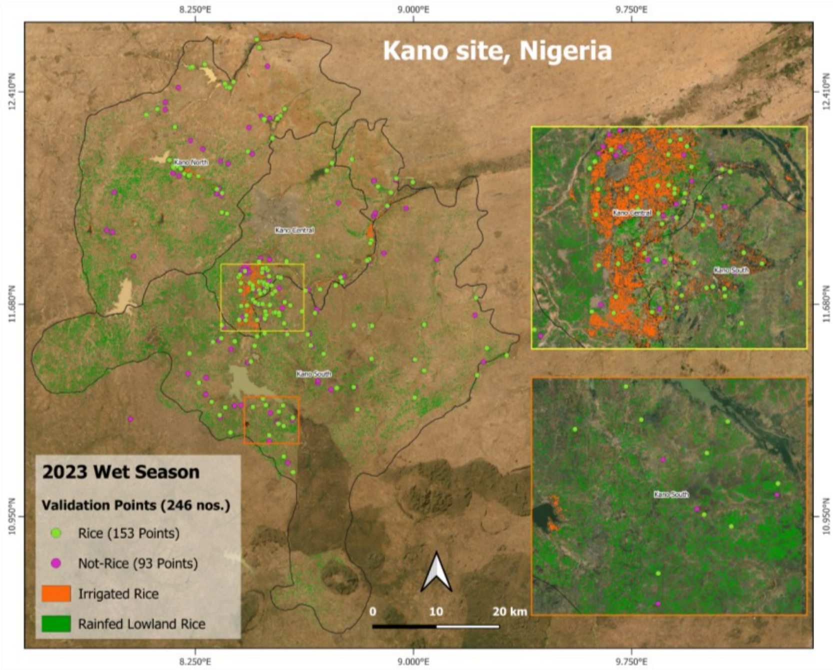

Figure 7.5. Spatial distribution of validation points (rice and non-rice) used for CRISP rice map validation in Kano, Nigeria during the 2023 wet season

Table 7.2. Confusion matrix for the rice area classification produced by CRISP and at the African continental level by Jiang et al. (2025) for the wet season of 2023, and in the Kano State, Nigeria. Both maps were compared to the 2023 field-collected points discussed in section 7.3.

CRISP Rice map					**Africa 20M Rice map (Jiang et al., 2025)**				
Predicted class from the map					Predicted class from the map				
		Rice	**Non-rice**	**Accuracy**			**Rice**	**Non-rice**	**Accuracy**
Actual class from survey	**Rice**	128	33	79.5%	Actual class from survey	**Rice**	6	147	3.9%
	Non-rice	16	84	84.0%		**Non-rice**	3	90	96.8%
	Reliability	88.9%	71.8%	**81.2%**		**Reliability**	66.7%	38.0%	**39.0%**
Average accuracy		81.8%			Average accuracy		50.3%		
Average reliability		80.3%			Average reliability		52.3%		
Overall accuracy		**81.2%**					**39.0%**		
Kappa index		0.62			Kappa index		-0.22		

To further interpret the CRISP results, the map was compared with the continental Africa 20m rice area map by Jiang et al. (2025) using the field dataset mentioned in section 7.3. The CRISP RA map significantly outperformed the 20m Africa map in Kano (Table 7.2). The Jiang´s 20 m Africa RA map reported an overall accuracy at only 39.0%, with a negative Kappa index (–0.22), reflecting very poor agreement with the field data. Rice areas were particularly under-detected, with only 3.9% rice mapping accuracy, compared to 79.5% in the CRISP map. Reliability values were also much lower: only 66.7% of predicted rice pixels were actually rice, and 38.0% of predicted non-rice pixels were correct. This led to a large underestimation of the rice areas, with only 41,892 ha of rice mapped across Kano in the Jiang RA map, compared to 206,139 ha for the CRISP RA map, considering both irrigated and rainfed together. Note in the map shown in 7.6 that the Jian's map tends to detect rice in rainfed area as large contiguous patches, which does not generally occur in the field unless irrigated schemes.

At the Senatorial District level (Table 7.3), spatial overlap and comparison analysis of rice fields further highlight the differences between the two products. In Kano South, both maps captured extensive rice areas; however, the CRISP map identified a much larger unique extent (103,266 ha; 75.6%) than the Africa 20 m map (26,533 ha; 19.4%), with limited overlap (6,722 ha; 4.9%). In Kano Central, the Africa 20 m product largely omitted the rice fields, including the highly productive and contiguous fields within the Kano River Irrigation Scheme (KRIS). CRISP alone captured almost the entire rice extent (33,999 ha; 99.8%), while Africa 20 m detected only 40 ha (0.1%). Similarly, in Kano North, CRISP mapped a larger rice extent (62,680 ha; 88.0%) than Africa 20 m (5,865 ha; 8.2%), with a small overlap of 2,692 ha (3.8%). Overall, across Kano State, CRISP uniquely mapped 199,945 ha (82.7%) of rice area, compared to 32,437 ha (13.4%) uniquely captured by the Africa 20 m map, with only 9,455 ha (3.9%) commonly mapped. These findings are consistent with the confusion matrix results, confirming that the Africa 20 m product substantially underestimates rice extent, especially in major irrigated landscapes such as KRIS, whereas CRISP provides a far more accurate and spatially complete representation.

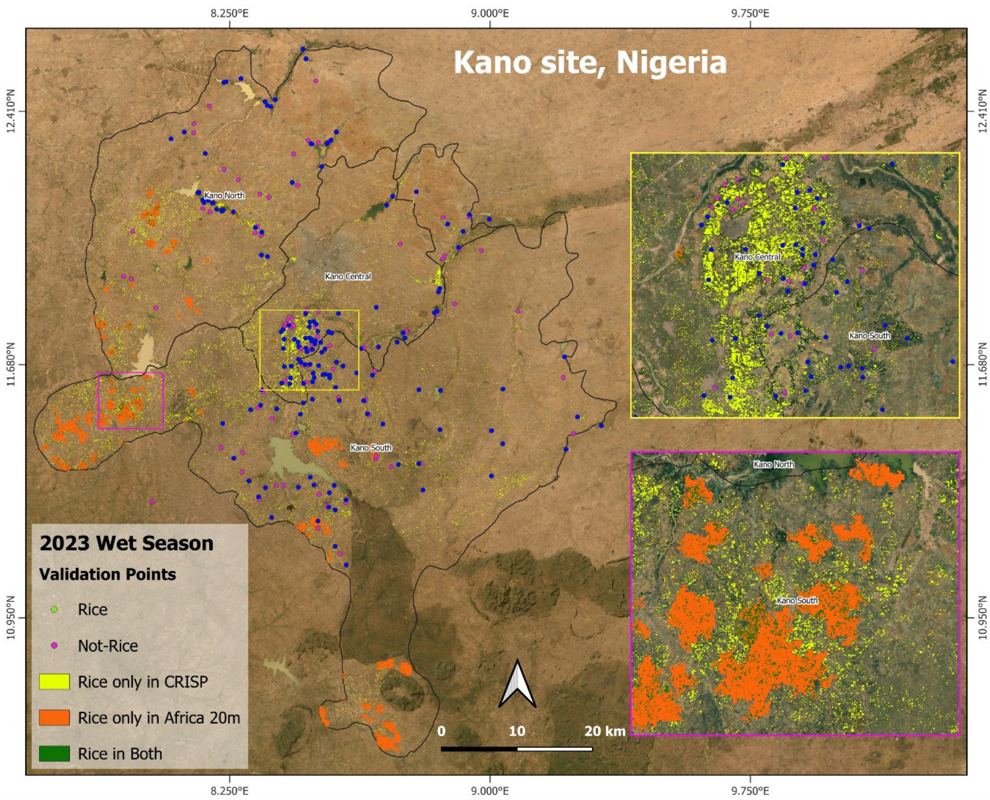

Figure 7.6. Comparison of the CRISP rice area map and rice area map produced at the African continental level by Jiang et al. (2025) for the wet season of 2023

Table 7.3. Sub-state level comparison of rice area mapped by the CRISP rice map and the Africa 20 m rice map (Jiang et al., 2025) for the 2023 wet season in Kano State, Nigeria

Senatorial District	Rice Area in ha and (%)			
	Only in CRISP	Only in Africa 20m	Both	Total
Kano South	103,266 (75.6)	26,533 (19.4)	6,722 (4.9)	1,36,520
Kano Central	33,999 (99.8)	40 (0.1)	41 (0.1)	34,080
Kano North	62,680 (88.0)	5,865 (8.2)	2,692 (3.8)	71,237
Kano State Total	**199,945 (82.7)**	**32,437 (13.4)**	**9,455 (3.9)**	**2,41,837**

7.4.2. Yield Validation

Table 7.3 shows the comparison of the CRISP yield estimates with the farmer's actual yield collected during the 2023 wet cropping season for both irrigated and rainfed areas. Overall, the yield estimates under the irrigated conditions (average 4.84 t/ha) closely match farmers' actual yields (average 4.74 t/ha), indicating a sound model performance. Most departments show small errors, with an overall RMSE of 0.32 t/ha and an NRMSE of 6.6%, which falls within a high-accuracy range. Departments such as Dawakin Kudu, Garun Mallam, and Warawara have particularly low error values, demonstrating excellent prediction accuracy. Although Bagwai shows a higher deviation between predicted and actual yields, the differences remain acceptable with a RMSE of less than 700 kg per hectare and a NRMSE of 14%. In general, the results suggest that the CRISP model reliably estimates crop yields across the irrigated areas, with only minor variations between predicted and actual performance.

However, in the rainfed conditions, results show a consistent pattern where CRISP yield estimates (average 3.47 t/ha) are notably lower than the actual farmer yields (average 4.70 t/ha) across all departments. This underestimation is reflected in the relatively high RMSE values, averaging 1.23 t/ha, and an overall NRMSE of 35%, indicating lower model accuracy under rainfed conditions compared to irrigated areas. Departments such as Kura and Gabasawa show the largest discrepancies, with NRMSE values of 45% and 37% respectively, suggesting substantial differences between predicted and actual yields. Warawara, despite having the largest sample size (52 fields), still shows a high NRMSE of 36%, reinforcing the trend that CRISP is less efficient in capturing yield variability under rainfed systems. Overall, these results suggest that rainfed environments —characterized by greater uncertainty in water availability and higher spatial variability, but also smaller and scattered fields —pose more challenge for CRISP yield prediction accuracy. Rainfed rice fields in West Africa such as in Nigeria are also often associated with trees which generate SAR signal noise and increase the level of error in the leaf area index product used to assess the crop development performance. The results in the rainfed areas shows that further calibration and refinement of the model are necessary to better capture the complex dynamics of rainfed production systems and improve prediction reliability in these highly variable conditions.

Table 7.3. Comparison of rice yield farmer's collected yield with yield estimates generated under CRISP in Kano State, Nigeria, during the 2023 wet season

Department	No. of Farmer's Field	CRISP Yield estimates (t/ha)	Average Farmer's yield (t/ha)	RMSE (t/ha)	NRMSE (%)
Irrigated					
Ajingi	21	4.77	4.23	0.54	11
Bagwai	7	4.92	4.24	0.68	14
Dawalin Kudu	6	4.76	4.74	0.01	0.3
Gabasawa	20	4.75	5.21	0.47	10
Garum Mallam	58	4.97	5.07	0.11	2
Kura	39	4.95	4.73	0.22	5
Warawara	41	4.78	4.98	0.20	4
		4.84	**4.74**	**0.32**	**6.6**
Rainfed					
Ajingi	27	3.41	4.52	1.11	32
Bagwai	11	3.51	4.48	0.97	28
Dawalin Kudu	26	3.41	4.55	1.14	33
Gabasawa	12	3.51	4.83	1.32	37
Garum Mallam	21	3.48	4.72	1.24	35
Kura	9	3.51	5.10	1.59	45
Warawara	52	3.47	4.72	1.25	36
		3.47	**4.70**	**1.23**	**35**

8. Multi-site validation

8.1. CRISP Rice Area Validation

The CRISP rice area products were validated across six major rice-producing regions in Asia and Africa, i.e. Srikakulam (Andhra Pradesh, India), Luzon (Philippines), Mwea Irrigation Scheme (Kenya), Senegal River Valley (Senegal), and Kano (Nigeria), covering both irrigated and rainfed rice ecosystems. Validation relied on independent field datasets, and accuracy metrics were computed using confusion matrices. Table 8.1 summarises the classification performance across all sites. Across sites, CRISP demonstrated strong and consistent performance, with an average overall accuracy (OA) of 86.9%, and ranging from 81.2% to 94.2%. The highest accuracy was observed in Srikakulam (Andhra Pradesh) with 94.2% OA, reflecting the well-structured irrigated landscape and clear phenological signatures of rice. Good performance was also recorded in Mwea, Kenya (92.7%) and Luzon, Philippines (84.9%), while accuracies in the African sites such as Senegal River Valley (81.5%) and Kano, Nigeria (81.2%) were slightly lower, consistent with their more heterogeneous landscapes, especially Nigeria. Rainfed systems such as the one dominating in Nigeria typically comprise fragmented fields (<1 ha), irregular planting schedules, and frequent tree cover interspersion, making rice and non-rice separation more challenging.

User's Accuracy (UA) values reveal an important pattern. Rice UA was consistently high across all sites, averaging 91.8%, and exceeding 85% in all regions. This shows that when CRISP labels a pixel as rice, it is highly likely to be correct, with minimal commission error. Non-Rice UA was lower, averaging 81.5%, and dropping to around 72-78% in Kano or SRV. These lower Non-Rice UAs indicate that rice fields are sometimes omitted (i.e., classified as non-rice), leading to conservative estimates of rice area. This is particularly common in regions with heterogeneous or tree-shadowed rice fields, spectral mixing along field edges, or where SAR multi-temporal filtering is sub-optimal. A common aspect between these two sites and seasons is some level of landscape complexity. SRV has no rainfed rice, but during the wet season rice is grown in both contiguous irrigated blocks and scattered smaller plots, mixed with rice-fallow areas where early rains often stimulate grass and weed growth. These vegetative covers produce SAR temporal signatures that closely mimic those of wet-season rice, leading to confusion and reduced separability during classification.

In several African sites, especially Senegal and Kano, the CRISP rice maps exhibited more localised salt-and-pepper patterns, even within contiguous irrigated blocks. These patterns can arise from (i) spatial heterogeneity, (ii) differences in acquisition timing relative to crop stages, (iii) environmental noise in Sentinel-1 SAR, and (iv) limitations in multitemporal speckle filtering. Despite these challenges, CRISP performed robustly, demonstrating adaptability to diverse agro-ecological and climatic conditions.

8.1.1. Flooded map validation

In addition to the ice area validation, the flood-map validation for the CRISP-derived Srikakulam flood layer during the 2018 Kharif cyclone showed an overall accuracy of 86.4%. The flooded class achieved 82.1% producer's accuracy and 88.7% user's accuracy, while the non-flooded class performed better with 91.3% producer's and 84.5% user's accuracy. The relatively lower accuracy for flooded pixels is likely due to short-duration inundation in many fields, water stagnation lasting fewer than three days and may not have been captured on the satellite acquisition day. Despite this limitation, the classification effectively detected major inundated areas and is suitable for district-level flood assessment and its integration with the rice area map.

Table 8.1. Summary of the rice area and flood mapping accuracy metrics obtained across the five CRISP test sites

Study Site	Rice Area (ha)	OA (%)	UA Rice (%)	UA Non-Rice (%)	Kappa
(i) Rice area maps					
Srikakulam, AP, India	214,181	94.2	95.5	91.9	0.88
Mwea Irrigation Scheme, Kenya	12,231	92.7	96.0	85.3	0.85
Senegal River Valley, Senegal	28,766	81.5	86.5	77.4	0.63
Kano, Nigeria	206,139	81.2	88.9	71.8	0.62
Luzon, Philippines	97,037	84.9	92.3	80.9	0.77
Average		**86.9**	**91.8**	**81.5**	**0.75**
(ii) Flood Map					
Study Site	**Flooded Area (ha)**	**OA (%)**	**UA Flooded (%)**	**UA Non-Flooded (%)**	**Kappa**
Srikakulam, AP, India	72,105	83.8	87.5	79.4	0.68

8.2. CRISP Yield Validation

The results for the assessment of the CRISP yield products are summarized in Table 8.2. Overall, the CRISP yield products yielded a reasonably good comparison with the yield reference data in some location but needs further validation in some. The average yield difference between CRISP and reference, ranged from 0.10 t/ha to 1.23 t/ha. The performance varied across sites and regions. The best performance was recorded in Kano for irrigated rice crops, followed by the irrigated SRV landscape in Senegal, with RMSE of 0.10 t/ha and 0.11 t/ha, respectively. In the Cagayan province, in the Philippines, the CRISP products detected the effect of the 2018-19 drought on the yield, but underestimated the yield as measured against the official government statistics by about 0.58 t/ha and 1.10 t/ha, during the 2017-2018 and 2018-2019 rice cropping season. The worst performance was recorded for the Mwea Irrigation Scheme with a RMSE of 1.23 t/ha. At the difference of the rice area where substantial field reference data were available, limited data could be used to validate the CRISP yield products. Crop Cut Experiments (field harvested samples) were used in Mwea and in SRV, although the number of surveyed fields was small in Senegal (N=8). In the case of the Nigeria Kano State, we use yield field data collected directly to the farmer at harvest time (indication of paddy rice bags collected per field). In Cagayan, Philippines, only the average yield recorded at Province level, published by the Philippine Statistics Authority was available. No yield map was generated for the site Srikakulam, in Andhra Pradesh.

The availability of quality reference data for validating or assessing yield crop estimates and maps is a common and well-known issue. Frequent challenges to obtain such data are associated with i) the inherent variability of agricultural systems at multiple scales, ii) issues with data quality, including misreporting of yield by farmers or extension officer as well as measurement or sampling errors, and iii) the high cost to collect field data. Reference data are scarce, and usually contain some degree of uncertainty, while its specific magnitude is mostly unknow. For instance, heavy rain, wind, and crop lodging occurred during the rice harvest in Mwea, main season 2023, when the CCE data were collected. These conditions may have introduced significant noise in the validating CCE dataset, although the errors are unknown. In the case of historical or post-event yield assessment (i.e. post-harvest) challenges are enhanced since the acquisition of field data through targeted and properly planned field data is no longer possible. In addition, government published data are often only available at large scale, e.g. Province in the case of Philippines, which limits the assessment of yield maps, while the protocols for compiling the field estimates are not always well documented.

The yield mapping model used by CRISP is based on the ORYZA crop growth model specifically design for the rice crop (https://sites.google.com/a/irri.org/oryza2000). The CRISP yield algorithm integrates maps derived from the remote sensing SAR data (including the rice area, crop establishment date or start-of-season, and Leaf Area Index) in the ORYZA crop model, and which are combined with non-remote sensing data on weather, soil conditions, dominant variety, and crop management data (Setiyono et al, 2029). For instance, the crop management data include information on fertilization, irrigation regime, or crop establishment method (transplanting or direct seeding). Like any model the outputs (e.g. yield) are sensitive to errors in inputs data, and to assumption or generalization made when considering the field conditions. For instance, inputted weather data are spatialized (CRISP uses mostly Copernicus AgERA5), and are limited by the resolution of the available weather datasets and costs. Other data generally are not available as spatialized layers, for instance the crop variety used or the access to irrigation water. In this case, the CRISP yield model makes assumption by defining dominant conditions which are generally valid for a specific region, e.g. most farmers in regions x uses variety y. Nevertheless, these conditions are a generalization, and discrepancies can be more or less important depending on local heterogeneity, leading to substantial uncertainties or errors, when compared to reference data.

Table 8.2. Summary of the yield mapping accuracy metrics obtained across the five CRISP test sites

Study Site	CRISP Yield (t/ha)	Reference Yield (t/ha)	RMSE (t/ha)	NRMSE (%)	Source of reference data
Srikakulam, AP, India	NA	NA	NA	NA	NA
Mwea Irrigation Scheme, Kenya	4.47	5.28	0.81	18	Crop cut experiments
Senegal River Valley, Senegal	4.14	4.03	0.11	2.7	Crop cut experiment
Kano, Nigeria, Irrigated	4.84	4.74	0.10	6.6	Farmer yield data
Kano, Nigeria, rainfed	3.47	4.70	1.23	35	Farmer yield data
Cagayan 2017-18, Philippines	4.18	4.76	0.58	14	Government statistics
Cagayan 2018-19, Philippines	3.23	4.34	1.11	34	Government statistics

9. Conclusion

This multi-site validation of the CRISP rice area, flood, and yield products confirms that the system is reliable and scalable for monitoring rice production across diverse agroecosystems in Asia and Africa. Across the five validation sites, CRISP achieved a mean overall accuracy of 86.9%, with irrigated systems such as Srikakulam (India) and Mwea (Kenya) recording accuracies above 90%. Even in ecologically more complex landscapes, including the Senegal River Valley (SRV) and Kano (Nigeria), the system maintained robust performance with accuracies above 80%, demonstrating its versatility in both structured and heterogeneous rice environments. The user's accuracy for rice was very high (average 91.8%), indicating strong reliability when CRISP identifies rice fields. Although still an overall good performer, Non-Rice user's accuracy was generally lower (on average 10%), especially in regions with fragmented field patterns, and mixed land-use covers, leading to rice field omission and possibly some rice area underestimation. Flood-map for Srikakulam during the 2018 cyclone event were well captured by CRISP mapping with an overall accuracy of 86.4%. Uncertainties arose from the short duration of water stagnation (often <3 days) in many fields, as compared to the 12-day satellite revisit cycle. Despite this limitation, the flood product provides reliable and timely inundation information for district-scale applications and integration with rice area maps, for assessing flood damage.

Yield validation showed larger variability across sites, influenced by the heterogeneity of field conditions, generalization of some input parameters, uncertainties in model parameterization, and limitation in availability and quality of reference and validation data. Average RMSE was 0.65 t/ha (range 0.1 to 1.23) and average NRMSE 18.4% (range 2.7 to 35%). While strong validation performance was achieved in irrigated systems such as Kano and Senegal River Valley, higher errors occurred in Mwea, Cagayan province, and in rainfed areas in Kano, where yield variability and sparse reference data pose challenges. Nevertheless, the CRISP yield model captured key spatial–temporal patterns, including drought-induced yield reductions and the contrast between high- and low-productivity areas. It is recommended in the future to implement assessment to current seasons (as opposed to historical), and implement more formal validation campaign, to consider the limitation of validation data.

Overall, the validation results demonstrate CRISP's strong potential as an operational tool for rice area mapping, flood impact assessment, and yield monitoring. Its multi-temporal SAR/optical fusion, phenology-driven workflow, and scalable modelling approach make it suitable for national and regional applications. Future enhancements, especially improved SAR preprocessing, better characterisation of mixed and complex rice ecologies like SRV, and expanded reference datasets, will further strengthen CRISP's accuracy and readiness for operational rice monitoring that supports crop insurance programs, policy decisions, climate resilience planning.

10. Reference

Busetto, L., Zwart, S.J. and Boschetti, M., 2019. Analysing spatial–temporal changes in rice cultivation practices in the Senegal River Valley using MODIS time-series and the PhenoRice algorithm. International Journal of Applied Earth Observation and Geoinformation, 75, pp.15-28.

Jiang, J., Zhang, H., Ge, J., Zuo, L., Xu, L., Song, M., Ding, Y., Xie, Y. and Huang, W., 2024. 20 m Africa Rice Distribution Map of 2023. *Earth System Science Data Discussions*, *2024*, pp.1-34.

Mane, I., Bassama, J., Diedhiou, P.M. and Mestres, C., 2024. Ways to improve the quality of local rice in Africa: comparison between physicochemical and sensory properties of rice consumed in Senegal. Nutrition & Food Science, 54(8), pp.1383-1395.

Setiyono, TD, ED Quicho, FH Holecz, NI Khan, G Romuga, A Maunahan, C Garcia, A Rala, J Raviz, F Collivignarelli, L Gatti, M Barbieri, DM Phuong, VQ Minh, QT Vo, A Intrman, P Rakwatin, M Sothy, T Veasna, S Pazhanivelan, MRO Mabalay, 2019. Rice yield estimation using synthetic aperture radar (SAR) and the ORYZA crop growth model: development and application of the system in South and South-east Asian countries. International Journal of Remote Sensing, 40(21), 8093-8124.

Tanaka, A., Diagne, M. and Saito, K., 2015. Causes of yield stagnation in irrigated lowland rice systems in the Senegal River Valley: Application of dichotomous decision tree analysis. Field Crops Research, 176, pp.99-107.

Gebremichael, M., Yue, H., Nourani, V. and Damoah, R., 2022. The skills of medium-range precipitation forecasts in the Senegal River basin. *Sustainability*, *14*(6), p.3349.

OMVS and IRD, 2002. Programme d'Optimisation et de Gestion des Réservoirs (POGR). Phase finale, rapport de synthese, Annexe 1 : Cultures de decrue, Dakar, Senegal (2002).

Van Oort, P.A.J., Balde, A., Diagne, M., Dingkuhn, M., Manneh, B., Muller, B., Sow, A. and Stuerz, S., 2016. Intensification of an irrigated rice system in Senegal: Crop rotations, climate risks, sowing dates and varietal adaptation options. *European Journal of Agronomy*, *80*, pp.168-181.

Dingkuhn, M., 1995. Climatic determinants of irrigated rice performance in the Sahel—III. Characterizing environments by simulating crop phenology. *Agricultural Systems*, *48*(4), pp.435-456.